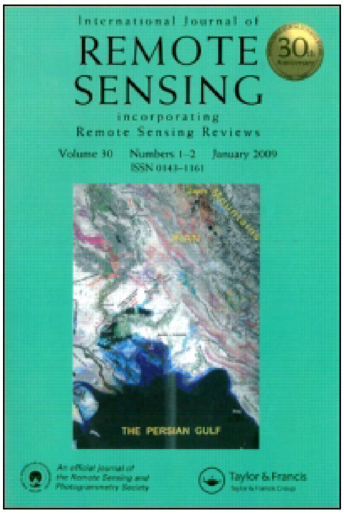

International Journal of Remote Sensing
Publication details, including instructions for authors and subscription information:
http://www.informaworld.com/smpp/title~content=t713722504

Global irrigated area map (GIAM), derived from remote sensing, for the end of the last millennium

Prasad S. Thenkabail [a]; Chandrashekhar M. Biradar [b]; Praveen Noojipady [c]; Venkateswarlu Dheeravath [d]; Yuanjie Li [c]; Manohar Velpuri [e]; Muralikrishna Gumma [f]; Obi Reddy P. Gangalakunta [g]; Hugh Turral [h]; Xueliang Cai [f]; Jagath Vithanage [f]; Mitchell A. Schull [i]; Rishiraj Dutta [j]
[a] Southwest Geographic Science Center, U.S. Geological Survey (USGS), Flagstaff, AZ 86001, USA [b] University of Oklahoma, Norman, OK 73019, USA [c] Department of Geography, University of Maryland College Park, MD 20742, USA [d] United Nations Joint Logistics Center, Juba, Sudan [e] Geographic Information Science Center of Excellence, South Dakota State University, Brookings SD 57007, USA [f] International Water Management Institute (IWMI), Colombo, Sri Lanka [g] National Bureau of Soil Survey and Land Use Planning, Indian Council of Agricultural Research (ICAR), Nagpur, India [h] On the Street Productions, North Carlton, Australia [i] Department of Geography, Boston University, USA [j] Indian Institute of Remote Sensing, Dehra Dun, India

Online Publication Date: 01 January 2009

International Journal of Remote Sensing
Vol. 30, No. 14, 20 July 2009, 3679–3733

Global irrigated area map (GIAM), derived from remote sensing, for the end of the last millennium

PRASAD S. THENKABAIL*†, CHANDRASHEKHAR M. BIRADAR‡, PRAVEEN NOOJIPADY§, VENKATESWARLU DHEERAVATH¶, YUANJIE LI§, MANOHAR VELPURI**, MURALIKRISHNA GUMMA††, OBI REDDY P. GANGALAKUNTA‡‡, HUGH TURRAL§§, XUELIANG CAI††, JAGATH VITHANAGE††, MITCHELL A. SCHULL¶¶ and RISHIRAJ DUTTA***

†Southwest Geographic Science Center, U.S. Geological Survey (USGS), 2255 N. Gemini Drive, Flagstaff, AZ 86001, USA
‡University of Oklahoma, 101 David L. Boren Blvd, Norman, OK 73019, USA
§Department of Geography, University of Maryland College Park, MD 20742, USA
¶United Nations Joint Logistics Center, Juba, Sudan
**Geographic Information Science Center of Excellence, South Dakota State University, Brookings SD 57007, USA
††International Water Management Institute (IWMI), 127 Sunil Mawatha, Colombo, Sri Lanka
‡‡National Bureau of Soil Survey and Land Use Planning, Indian Council of Agricultural Research (ICAR), Nagpur, India
§§On the Street Productions, 28 Newry Street, North Carlton, Melbourne 3054, Australia
¶¶Department of Geography, Boston University, USA
***Indian Institute of Remote Sensing, Dehra Dun, India

(*Received 26 December 2007; in final form 12 June 2008*)

A Global Irrigated Area Map (GIAM) has been produced for the end of the last millennium using multiple satellite sensor, secondary, Google Earth and groundtruth data. The data included: (a) Advanced Very High Resolution Radiometer (AVHRR) 3-band and Normalized Difference Vegetation Index (NDVI) 10 km monthly time-series for 1997–1999, (b) Système pour l'Observation de la Terre Vegetation (SPOT VGT) NDVI 1 km monthly time series for 1999, (c) East Anglia University Climate Research Unit (CRU) rainfall 50 km monthly time series for 1961–2000, (d) Global 30 Arc-Second Elevation Data Set (GTOPO30) 1 km digital elevation data of the World, (e) Japanese Earth Resources Satellite-1 Synthetic Aperture Radar (JERS-1 SAR) data for the rain forests during two seasons in 1996 and (f) University of Maryland Global Tree Cover 1 km data for 1992–1993. A single mega-file data-cube (MFDC) of the World with 159 layers, akin to hyperspectral data, was composed by re-sampling different data types into a common 1 km resolution. The MFDC was segmented based on elevation, temperature and precipitation zones. Classification was performed on the segments.

Quantitative spectral matching techniques (SMTs) used in hyperspectral data analysis were adopted to group class spectra derived from unsupervised

*Corresponding author. Email: pthenkabail@usgs.gov. Formerly of International Water Management Institute (IWMI), 127 Sunil Mawatha, Colombo, Sri Lanka.

International Journal of Remote Sensing
ISSN 0143-1161 print/ISSN 1366-5901 online © 2009 Taylor & Francis
http://www.tandf.co.uk/journals
DOI: 10.1080/01431160802698919

classification and match them with ideal or target spectra. A rigorous class identification and labelling process involved the use of: (a) space–time spiral curve (ST-SC) plots, (b) brightness–greenness–wetness (BGW) plots, (c) time series NDVI plots, (d) Google Earth very-high-resolution imagery (VHRI) 'zoom-in views' in over 11 000 locations, (e) groundtruth data broadly sourced from the degree confluence project (3 864 sample locations) and from the GIAM project (1 790 sample locations), (f) high-resolution Landsat-ETM+ Geocover 150 m mosaic of the World and (g) secondary data (e.g. national and global land use and land cover data). Mixed classes were resolved based on decision tree algorithms and spatial modelling, and when that did not work, the problem class was used to mask and re-classify the MDFC, and the class identification and labelling protocol repeated. The sub-pixel area (SPA) calculations were performed by multiplying full-pixel areas (FPAs) with irrigated area fractions (IAFs) for every class.

A 28 class GIAM was produced and the area statistics reported as: (a) annualized irrigated areas (AIAs), which consider intensity of irrigation (i.e. sum of irrigated areas from different seasons in a year plus continuous year-round irrigation or gross irrigated areas), and (b) total area available for irrigation (TAAI), which does not consider intensity of irrigation (i.e. irrigated areas at any given point of time plus the areas left fallow but 'equipped for irrigation' at the same point of time or net irrigated areas). The AIA of the World at the end of the last millennium was 467 million hectares (Mha), which is sum of the non-overlapping areas of: (a) 252 Mha from season one, (b) 174 Mha from season two and (c) 41 Mha from continuous year-round crops. The TAAI at the end of the last millennium was 399 Mha. The distribution of irrigated areas is highly skewed amongst continents and countries. Asia accounts for 79% (370 Mha) of all AIAs, followed by Europe (7%) and North America (7%). Three continents, South America (4%), Africa (2%) and Australia (1%), have a very low proportion of the global irrigation. The GIAM had an accuracy of 79–91%, with errors of omission not exceeding 21%, and the errors of commission not exceeding 23%. The GIAM statistics were also compared with: (a) the United Nations Food and Agricultural Organization (FAO) and University of Frankfurt (UF) derived irrigated areas and (b) national census data for India. The relationships and causes of differences are discussed in detail. The GIAM products are made available through a web portal (http://www.iwmigiam.org).

1. Introduction, background and rationale

The population of the world is now approaching 6 billion and is expected to near 8 billion by 2025. Some estimate that, to meet future food demand, at least another 2000 km^3 of water (equivalent to the mean annual flow of 24 additional Nile rivers) will be needed (Postel 1999). Irrigation is widely thought to provide 40% of the world's food from around 17% of the cultivated area. It accounts for 2–4% of diverted water in Canada, Germany and Poland, but is an impressive 90–95% in Iraq, Pakistan, Bangladesh, Sudan, Kyrgyzstan and Turkmenistan (Merrett 2002). However, the actual areas irrigated and their spatial distributions can be further improved using modern remote sensing data. Given that nearly 80% of all freshwater used by humans is for irrigation, the importance of irrigated areas cannot be overemphasized.

Following the end of the Second World War and a period of decolonization, there was a boom in irrigation development, particularly in Asia, which coincided with strongly motivated nation building, poverty alleviation and famine eradication. In this era, a key developmental agenda for many countries was the construction of large and small dams and river diversions to abstract and store water for agriculture. Over 40 000 large dams (>15 m in height) irrigate about 30–40% of the world's irrigated areas (www.dams.org) and are complemented by an estimated 800 000 smaller dams. Irrigated areas increased at about 2.6% per annum from a modest 95 million hectares (Mha) in the early 1940s to between 250 and 280 Mha in the early 1990s (Van Schilfgaarde 1994, Seckler *et al.* 2000, Siebert *et al.* 2005a,b, 2006). These are massive increases when compared with the earlier era when irrigated areas increased form a meagre 8 Mha in year 1800 to 95 Mha by 1940. Since the 1980s, there has been a progressive decline in public and international donor funding for irrigation, which has been replaced in many countries by the private development of groundwater irrigation based on availability of cheap drilling and pumping technologies. The number of groundwater wells in India, for example, are now estimated at 26 million, followed by the USA (16 million), China (3.4 million), Bangladesh (800 000), Pakistan (700 000), Germany (500 000) and South Africa (500 000) (see Shah *et al.* 2003, 2004, Endersbee 2005, www.wellowner.org,). Yet, the areas irrigated from groundwater are often missing from the statistics and maps produced (e.g. the Central Board of Irrigation and Power (CBIP) 1994 map). At present, globally, the irrigated landscape remains very dynamic. Although the annual rate of increase of irrigated areas has slowed to about 1%, this still represents an increase of between 3 and 4 Mha each year. There is a smaller corresponding annual loss of irrigated area to salinity and water logging, as well as abandonment of uneconomic projects. Countries, such as China and India, continue to build large multi-purpose dam projects that also supply water for irrigation. In sub-Saharan Africa, irrigation is perennially seen as having unfulfilled potential. Elsewhere in the world, there are moratoria on dam building and even on the decommissioning of dams in western USA.

There remains considerable uncertainty about the exact extent or area, cropping intensity and the precise spatial distribution of irrigated areas in different parts of the world due to both the absence of systematic irrigated area mapping at global level and systematic problems in underreporting and over-reporting of irrigation in different contexts (e.g. groundwater). Indeed, often the irrigated area statistics do not include minor or informal irrigated areas (e.g. groundwater, small reservoirs and tanks). Yet, in many countries, minor irrigated areas are very significant and even exceed the major irrigated areas (e.g. major and medium reservoirs created by building large dams and barriers) (MoWR 2005). The United Nations Food and Agriculture Organization (FAO)/University of Frankfurt (UF) study on irrigated areas of the world (Döll and Siebert 2000, Siebert *et al.* 2005a,b, 2006) is primarily based on FAO AQUASTAT statistics, which, in turn, is based on census statistics from individual nations. It provides estimates of area ‘equipped’ for irrigation (but not necessarily irrigated) in the world as 278.8 Mha around year 2000 (see Siebert *et al.* 2006), which is about 19% of the total croplands (1.5 billion ha) around year 2000. Irrigated areas are estimated, rather coarsely, in global land use classifications (DeFries *et al.* 1995, 1998, 2000a,b, Loveland *et al.* 2000, Bartholome and Belward 2005) derived from remote sensing, which are usually focused on other objectives, such as forestry, rangelands and rain-fed croplands.

There will be other causes for uncertainty in irrigated areas in the near future. Rain-fed croplands are identified as areas for productivity increases (CA 2007) and may yet have an impact on limiting expansion of irrigated areas in the coming decades. If serious advances are made in using less water to produce more food (better water productivity), irrigated areas may drastically change. Spatial distribution of irrigated areas may also change if the concept of 'virtual water trade' (where countries with surplus water grow food and export to water-deficit countries for other trade benefits) takes hold. Irrigated croplands are significantly being converted to bio-fuel farms in certain parts of the world. Genetic engineering may help increase yields, but is increasingly questioned by environmental activists and more ecologically sensitive governments. The irrigated landscape of the world will be shaped increasingly by the effects of competition for water from other sectors, notably urban and rural domestic water supply and industrial needs. Groundwater overdraft may ultimately exhaust and/or substantially reduce irrigated areas in the Ogallala aquifer in the mid-western USA, northeast China and most of India. Reserving and reallocation of flows for environmental and health purposes will, in the end, place even greater competing demands in terms of water volume. River basins are becoming over-allocated, as in the case of the Krishna basin in India leading to reallocation of water and change in spatial distribution of irrigated areas (Biggs *et al.* 2006). Climatic change will impose additional challenges that will reshape the irrigated landscape through changes in snowmelt runoff and rainfall.

The greater the certainty in area estimation and geographic precision, the greater the certainty in water-use calculations and food-production planning. For example, in India, in order to produce 1 kg of rice, 3700 l of water are evaporated, whereas 1 kg of wheat evaporates 2560 l and 1 kg of maize evaporates 4350 l (http://en.wikipedia.org/wiki/Virtual_water, http://www.clw.csiro.au/issues/water/water_for_food.html). In China, 1 kg of rice, wheat and maize require much lesser amounts of water at 1370, 1280 and 1190 l, respectively. In the USA, this comes to 1920, 1390 and 670 l for rice, wheat and maize, respectively. In comparison, 1 kg of beef requires 14 379 l in India, 12 600 l in China, and 10 060 l in the USA.

Based on the above needs and possibilities, the International Water Management Institute (IWMI) initiated a Global Irrigated Area Mapping (GIAM) project. We used the availability of a wide range of increasingly sophisticated remotely sensed images and techniques to reveal vegetation dynamics that:

- define more precisely the actual area and spatial distribution of irrigation in the world;
- elaborate the extent of multiple cropping over a year, particularly in Asia, where two or three crops may be planted in one year, but where cropping intensities are not accurately known or recorded in secondary statistics; and
- develop methods and techniques for consistent and unbiased estimates of irrigation over space and time for the entire world.

Thereby, the overarching goal of this research was to create a GIAM by developing repeatable and robust methods and techniques of analysis using remote sensing data. Two types of irrigated areas will be reported: (1) TAAI, which does not consider the intensity of irrigation and (2) annualized irrigated areas (AIA), which consider the intensity of irrigation by summing areas from different seasons and perennial crops such as plantations. Specific emphasis will be placed on mapping classes of: (i) major irrigation from large and medium surface-water reservoirs and (ii) minor irrigation from groundwater, small reservoirs and tanks. Through this effort, it was envisaged to: (a) provide irrigated area statistics and maps for every country in the world, (b) determine accuracies and uncertainties in area estimates and (c) compare them with results from FAO/UF (Siebert *et al.* 2006) and national statistics. The study is expected to provide baseline remote sensing based data and products on global irrigated areas at the end of the last millennium.

2. Methods and materials

First, we describe the data sets and the reasons for choosing them. This will be followed by the methods used.

2.1 *Data used in the creation of the IWMI's GIAM*

The process used in this study starts with a number of publicly available primary and secondary data sets, which are processed into one single large 159 layer time series file, known as a mega-file data-cube (MFDC) (see illustrations in figure 1 and table 1), similar to a hyperspectral data-cube (Thenkabail *et al.* 2004a,b). The drop-down menu illustrates how the data layers are composed in the MFDC (e.g. figure 1), which consisted of 144 Advanced Very High Resolution Radiometer (AVHRR) 10 km layers for the years 1997–1999 (4 bands * 3 years * 12 months; with red, near-infrared, thermal infrared band number 4 and a scaled Normalized Difference Vegetation Index (NDVI) band), 12 Système pour l'Observation de la Terre vegetation (SPOT VGT) 1 km data layers (see table 1), each for every month of the year 1999, a single layer of Global 30 Arc-Second Elevation Data Set (GTOPO30) digital elevation model (DEM) 1 km, mean annual rainfall for 40 years at 50 km resolution and AVHRR-derived forest cover at 1 km. All layers in the MFDC were resampled to 1 km to analyse data at the SPOT VGT resolution. This increases the data volume, but makes it possible to view the data characteristics such as band reflectivity, the NDVI of different sensors, precipitation, elevation and temperature at a click of a mouse, instantaneously, for any given point in the world. However, since the overwhelming numbers of data layers were from AVHRR, the final product is referred to as a nominal 10 km. Co-registration of the MFDC required very careful synthesis as a result of inherent difficulties associated with varying resolutions: AVHRR, 10 km; SPOT VGT, 1 km; Japanese Earth Resources Satellite-1 (JERS-1) Synthetic Aparture Radar (SAR), 100 m; Precipitation, 50 km; and GTOPO30, 1 km. Co-registration was achieved using ground control points (GCPs) matched between the two different types of images (e.g. AVHRR versus SPOT) resampled to 1 km. Polynomial warping with nearest neighbour resampling was preferred because of its simplicity. An evaluation was conducted using spectral values between the original and wrapped images from specific locations. The results showed that the resampled AVHRR and SPOT images retained spectral integrity and other data, such as rainfall (mm yr^{-1}) and elevation (m), had the same values in specific geographic locations in comparison to their original resolution data. The multi-sensor data sets widely vary in their spectral, spatial and radiometric characteristics, have gone through complex normalization algorithms to correct for issues such as Sun elevation, Earth–Sun distance, sensor calibration coefficients and cloud and haze removal. All this will add its own uncertainties in irrigated area estimates. Recognizing this, the coarser resolution time series used in this study from the AVHRR pathfinder and the SPOT VGT are supported by: (a) high-quality secondary spatial data such as GTOPO30, precipitation and temperature, (b) JERS-1 SAR, (c) high resolution 'groundtruth' from Landsat Geocover, Google Earth and (d) actual groundtruth from degree confluence and GIAM projects. In addition, sophisticated and rapid access to groundtruth data from Google Earth

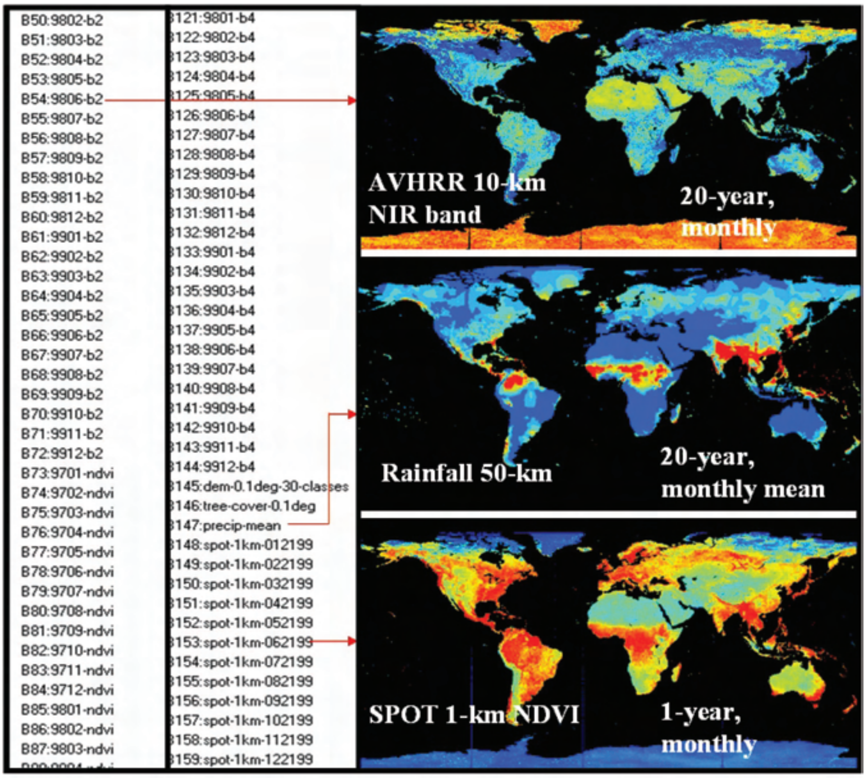

(a)

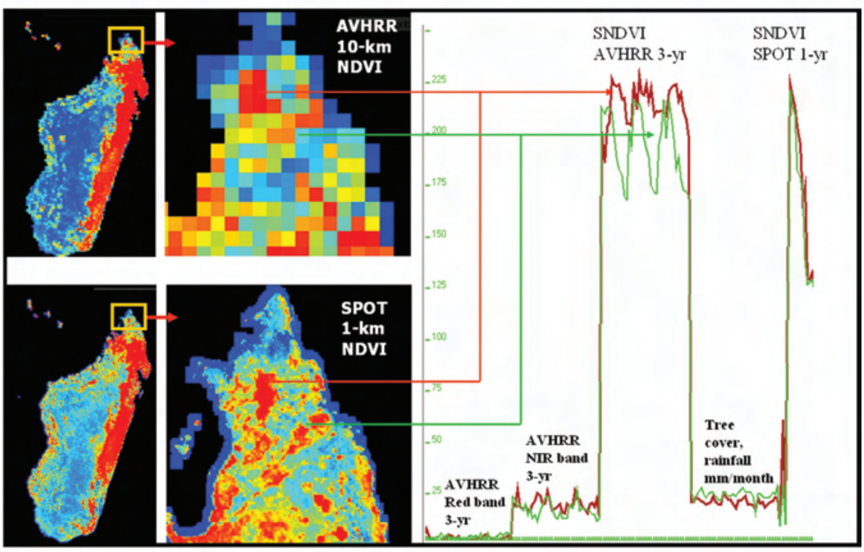

(b)

Figure 1. Mega-file data cube (MFDC): (a) A single global file MFDC of 159 data layers, consisting of time-series primary and secondary satellite sensor data from various sources. (b) illustrates the mega-file, at any given point, providing characteristics of all the 159 data layers. **Note**: SNDVI = scaled normalized difference vegetation index, AVHRR = Advanced Very High Resolution Radiometer, SPOT = Système pour l'Observation de la Terre Vegetation, NIR = near-infrared. X-axis provides time-series values of MFDC month after month. Y-axis represents AVHRR or SPOT digital numbers of bands or SNDVI in 8-bits. The rainfall in mm\month and tree cover class numbers. B50:9802-b2: represents band 50 in the MFDC which is for year 1998, month 2, and band 2.

Table 1. Characteristics of the Mega-file datasets used in the study. The characteristics of the primary satellite sensor time-series data and the secondary datasets (see Table 1a) as well as other datasets (see Table 1b).

Table 1a

Band number Or primary source (#)	**Wavelength range** (μm)	**Duration** (years)	**Number of bands**[1] (#)	**Data final format radiometry** (percent: for reflectance)	**Range Z-scale** (dimensionless)
Satellite sensor data					
AVHRR 10-km					
Band 1 (B1)	0.58 – 0.68	1997–1999	36	reflectance @ ground, 8-bit	0–100
Band 2 (B2)	0.73–1.1	1997–1999	36	reflectance @ ground, 8-bit	0–100
Band 4 (B4) (top-of-atmosphere)	10.3–11.3	1997–1999	36	Brightness temperature	160–340
NDVI	(B2−B1)/(B2+B1)	1982–2000	36	unitless, 8-bit scaled NDVI	−1 to +1
Secondary data					
GTOPO30 1-km					
one-band	DCW, DTM, and others[2]	1 time	1	meters, 16-bit	−1 to + 1
Rainfall 1-km					
one-band	Mean of monthly 40-years	1961–01	1	mm, 16-bit	0–65536
Forest cover 1-km					
one-band	None	1992–93	1	class names, 8-bit	0–256

Table 1b

1. Band 1, 2, NDVI	same as above	1981–2001	239*		
2. SPOT 1-km[2]					
NDVI	(B3−B2)/(B3+B2)	1999	12	unitless, 8-bit scaled NDVI	−1 to +1
3. JERS SAR 100-m					
one-band	L-band;24.5 cm	Jan. –Mar 1996	1	unitless, 8-bit	0–256
		Oct-Nov 1996	1	unitless, 8-bit	0–256

Note: 1 = for satellite sensor data: 36 bands from 3 years with 1 band per month. 2 = DCW = digital chart of the World, DTM = digital terrain model.
* = animations of the irrigated area classes were run for the entire AVHRR time-series data to help understand the change history of the class.
There was data for 239 months in 19 years (July 1981– September 2001). September-December 1994 data was not acquired due to failure of the satellite.

'zoom-in views' of very-high-resolution imagery (VHRI), degree confluence data and actual groundtruth data. Combinations of these data sets, at global levels, make it feasible to map and study irrigated areas and help determine their uncertainty. The following sections provide a brief description of each of the data sets, which are summarized in detail in table 1. Readers interested in further details of these data may look into detailed documentation in the web portals of the GIAM project (http://www.iwmigiam.org), IWMI's data storehouse pathway or IWMIDSP (http://www.iwmidsp.org) and in various references (Thenkabail *et al.* 2005, 2006, 2007a,b, Biggs *et al.* 2006).

2.2 *Primary remote sensing datasets*

2.2.1 AVHRR data characteristics. The monthly time-composite NOAA AVHRR 0.1° data were obtained from the NASA Goddard DAAC site (www.daac.gsfc.gov/data/data set/AVHRR). This 'Pathfinder' data set has gone through many stages of calibration and recalibration (Kidwell 1991, Rao 1993a,b, Agbu and James 1994, Smith *et al.* 1997) and normalization (Fleig *et al.* 1984, NGDC 1994, Kogan and Zhu 2001), making it a high-quality science data set and minimizing the known limitations (see Eidenshink and Faundeen 1994, Loveland *et al.* 1999, 2000, http://daac.gsfc.nasa.gov/www/islscp/). The original scaled 16 bit and 8 bit data have been converted to three primary variables: (a) at-ground reflectance, (b) top of atmosphere brightness temperature and (c) NDVI. These parameters were derived using calibration parameters (Abu and James 1994, Smith *et al.* 1997). In the GIAM project, the monthly data of AVHRR band 1, band 2, thermal band 4 and NDVI maximum value composite (MVC; Holben 1986) were used for the years 1997–1999 (figure 1 and table 1).

2.2.2 SPOT data characteristics. The SPOT VGT (Lissens *et al.* 2000) 1 km NDVI 10 day synthesis for year 1999 was downloaded for the entire world (http://free.vgt.vito.be/), converted to monthly MVCs (Holben 1986, Thenkabail *et al.* 2005, Biggs *et al.* 2006) and used in this study (figure 1 and table 1).

2.2.3 JERS-1 SAR-derived forest cover. Mapping irrigated areas in rain forests is more complex than in other parts of the world as a result of forest fragmentation, significant cloud cover and the presence of natural wetlands. Therefore, we obtained 100 m resolution JERS-1 SAR L-band (24.5 cm wavelength) imaging radar tiles (http://southport.jpl.nasa.gov/GRFM/, Saatchi *et al.* 2000) in conjunction with AVHRR, SPOT and secondary data for South America to assist us in mapping areas in major rain forest areas. These images were classified separately and the class backscatter coefficients were determined and linked to groundtruth knowledge to understand irrigation versus no irrigation. Normalized radar cross section (sigma0) is measured in decibels (dB) and is used for quantitative characterization of land cover and land use (Saatchi *et al.* 2000). Typical values of sigma0 for natural surfaces range from +5dB (very bright) to −40dB (very dark) (Saatchi *et al.* 2000). Qualitatively, flooded irrigated lands will appear bright, and drier targets will appear dark. Young vigorous irrigated crops appear very bright. The smooth body of water will act as a flat surface and reflect incoming pulses away from a target; these bodies will appear dark. Forests appear medium bright and clear-cut areas very dark.

2.3 *Mask data for stratification*

Secondary data sets (table 1) in the mega-file are used to stratify or segment the world into characteristic regions based on precipitation, elevation, temperature and forest cover. The MFDCs are created for each of the seven segments listed below, classified and investigated for presence or absence of irrigation. The seven global masks are:

- precipitation less than 360 mm yr^{-1} (PLT360);
- precipitation greater than 2400 mm yr^{-1} (PGT2400);
- temperature less than 280 K yr^{-1} (TLT280);
- forest cover greater than 75% canopy cover (FGT75);
- special forest SAR (FSAR);
- elevation higher than 1500 m (EGT1500); and
- all other areas of the world (AOAW) that are outside the above six segments.

The above seven segments cover the area of the entire terrestrial world. MFDCs were composed for each of the above seven segments. The segments were used to generate class spectra using unsupervised classification. The classes were then further investigated to identify and label them. Segmentation helps in focusing on particular precipitation, temperature, forest cover and elevation zones and helps us in analysing areas within these zones.

2.3.1 Climate Research Unit (CRU) precipitation. The 40 year (1961–2000) monthly, 0.5°, interpolated precipitation data were obtained from Dr Tim Mitchell of the CRU, University of East Anglia, UK (Mitchell *et al.* 2003, http://www.cru.uea.ac.uk/~timm/index.html). Two precipitation segments, one where precipitation is less than 360 mm yr^{-1} (PLT360) and another where precipitation is greater than 2400 mm yr^{-1} (PGT2400), were used in this study. The segment with less than 360 mm yr^{-1} (PLT360) identifies areas where any green cropland vegetation has a very high likelihood of being irrigated, since average evaporation rates of 30 mm $month^{-1}$ will be considerably less than evaporative demand. This segment will help focus on identifying irrigated and non-irrigated classes in the arid and semiarid areas and deserts. By contrast, the segment with precipitation over 2400 mm yr^{-1} (PGT2400) mainly identifies the rain forest areas of the world, although there are considerable areas of irrigation in this segment within the southeast Asian lands, identified based on protocols discussed later.

2.3.2 Temperature segment. The 20 year mean AVHRR thermal band 4 data were used to segment the world for areas less than 280 K. Where the mean temperature is below 280 K on average (TLT280), it is too cold for agriculture, and irrigation is not likely to be found there. However, some northern hemisphere areas have low average temperatures but short summer seasons (May–October) in which supplemental irrigation is actually practiced. Thereby, even in this zone classes are created and identified.

2.3.3 Forest cover data. A forest cover of greater than 75% (FGT75) was used as one of the segments. Areas of very high forest cover imply that these areas are unavailable for cultivation and the likelihood of irrigation is even less. Nevertheless, the MFDC of FGT75 is classified and class identification and labelling process followed. Forest cover was derived from the 1992 AVHRR 1 km data by the University of Maryland (DeFries and Townshend 1994, DeFries *et al.* 2000a,b). If forest density is greater than 75%, it is also rare that there will be any irrigation, due to high rainfall and limited infrastructure. There is likely to be slash-and-burn agriculture in small fragments. This mask is complemented by a rain-forest mask derived from the JERS-1 SAR (FSAR) imagery, in order to better identify other land use fragments at higher resolution within the rain forest areas, including where there might be irrigation. The rainforest mask implies that the areas of rainforests are segmented and analysed separately and includes the use of JERS SAR data apart from all other data used globally. The JERS SAR data was not used in areas outside the rainforests.

2.3.4 GTOPO30 1 km DEM. The GTOPO30 is a 1 km global elevation data derived from eight sources (USGS 1993, Verdin and Greenlee 1996, Verdin and Jenson 1996, Tucker *et al.* 2005) and were used to segment the world for elevations higher than 1500 m (EGT1500). There is a lower likelihood of irrigation above an elevation of 1500 m, although there are certainly hill irrigation systems in the Andes, Himalayas and the Philippines at higher elevations. The classes of the EGT1500 are likely to be dominated by forests as likely land cover, but should be separable from irrigation and agriculture due to their continuous vegetation signature using the protocols described below.

Finally, the segment 'AOAW' focuses on where there are few biophysical constraints to irrigation and shows where we are most likely to find it in various forms. Overall, the segments help us to focus interpretation; but the presence or absence of irrigation is investigated in detail in every segment. Even in segments with very low likelihood of irrigation, detailed investigations were carried out to track any remnants of irrigation.

3. Overview of methods

An overview summary of the methods and analytical techniques are shown in figure 2. The basic process begins with segmenting the MFDC (figure 1 and table 1) into characteristic temperature, elevation and precipitation regions that makes it easier for analysis, generating class spectra through classification by classifying the 159 layer MFDC for each of the seven segments, grouping class spectra based on class similarities and/or by comparing them with target spectra, rigorous protocols for class identification and labelling that include use of large volumes of groundtruth data and the use of VHRI, resolving mixed classes through specifying decision trees and spatial modelling, standardized class naming and class name verification and establishing innovative methods for irrigated area calculations and accuracy assessments. These processes are described in the following sections and presented in further detail in a research report (Thenkabail *et al.* 2006, http://www.iwmigiam.org).

The MFDC retains the integrity of each data layer and unlike data fusion does not merge data. In contrast to data fusion, the MFDC retains a series of data layers, akin to hyperspectral data layers, each with its own characteristics but resampled to 1 km. The various data layers are geographically precise.

3.1 *Class spectra generation through unsupervised classification*

The mega-files of each of the seven segments are processed using unsupervised ISOCLASS *k*-means classification (Tou and Gonzalez 1975, Leica 2005) to produce a large number of class spectra. In each segment, we began with 250 classes as a start. In some smaller segments or more homogeneous segments (e.g. segment TLT280), the maximum number of classes produced by the *k*-means algorithm was less than 250 classes, even when we specified 250 classes.

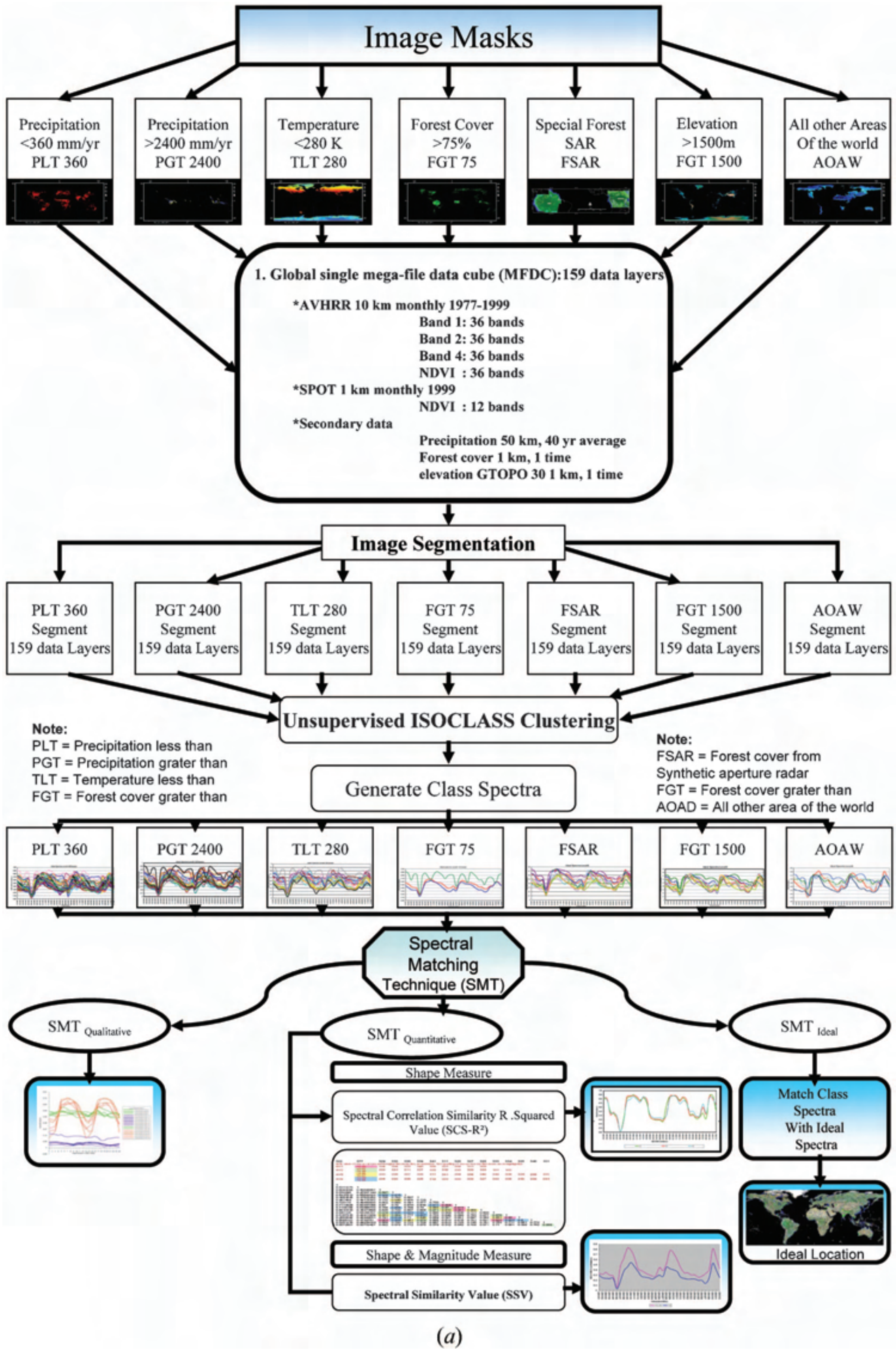

Figure 2. Methodology for mapping global irrigated areas (GIAM). The flow-charts provide an overview of the GIAM methodology.

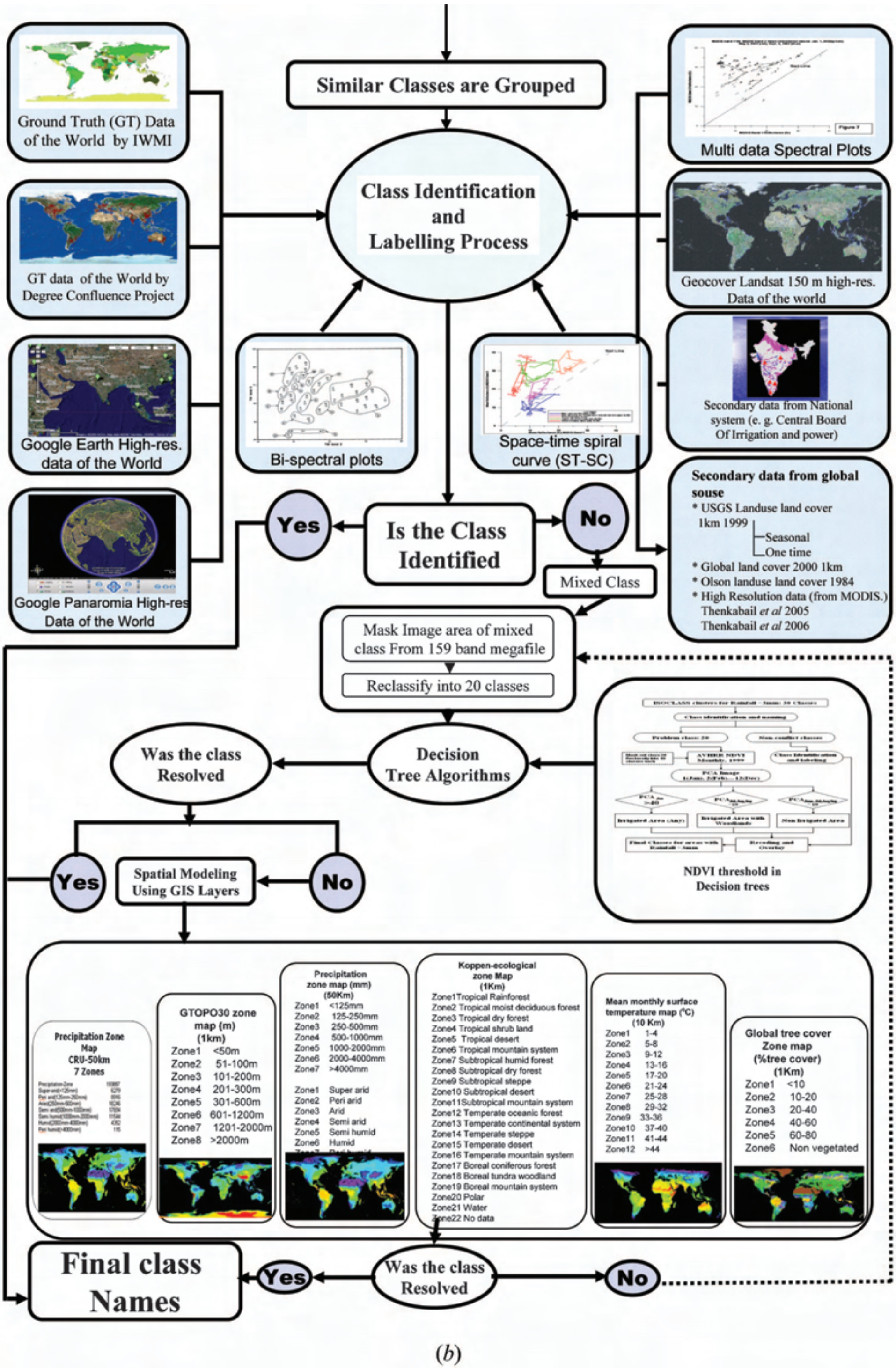

(b)

Figure 2. (Continued.)

3.2 *Class grouping through Spectral Matching Techniques (SMTs)*

In more localized applications, it is common to undertake groundtruth to identify and label the classes generated using the ISOCLASS algorithm. However, at the global scale, this is not possible due to enormous resources required to cover vast areas to identify and label classes. So as a first step, SMTs (Farrand and Harsanyi 1997, Bing *et al.* 1998, Granahan and Sweet 2001, Schwarz and Staenz 2001, Shippert 2001, Homayouni and Roux 2003, Thenkabail *et al.* 2007a) were used to group classes. Time-series of NDVI (e.g. sample illustration in figure 3) or other metrics are analogous to spectra, where time is substituted for wavelength. The principle in spectral matching is to match the shape, or the magnitude or (preferably) both to an ideal or target spectrum (commonly known as a pure class or 'end-member') (Thenkabail *et al.* 2007a). In cases where the class does not have matching ideal spectra, the class identities are investigated through the methods described below in order to label them.

Two quantitative SMTs, to group classes, adopted in this study were (Thenkabail *et al.* 2007a):

(a) Spectral Correlation Similarity (SCS), which is the shape measure and
(b) Spectral Similarity Value (SSV), which is the shape and magnitude measure.

The range of SCS R^2 values (where R^2 is the coefficient of determination) lies between -1 and $+1$, but negative values have no meaning in this application. The higher the positive value, the greater the similarity. The normal range of SSV is from 0 to 1.415. The smaller the SSV value, the greater the similarity of classes. The process of grouping classes based on SCS R^2 values is illustrated in figure 3. Figure 3(*a*) shows how the classes group based on similar SCS R^2 values. Figure 3(*b*) shows the results of grouping similar spectra for double crop irrigation, continuous forest cover and bare or fallow soils. The SMTs perform two key functions: (*a*) first, they group data of similar classes (e.g. figure 3) and (*b*) second, they help identify classes by matching the class spectra, with ideal or target spectral data bank, which is generated based on precise groundtruth knowledge.

In this paper, we use SMTs extensively to: (i) group a large number of classes to a few distinct groups of classes (e.g. figure 3) and (ii) group and label classes by comparing the group of similar classes of class spectra with ideal/target spectra from the precise groundtruth locations. The reader can refer to Thenkabail *et al.* (2007a) for a detailed discussion on the application of SMTs in irrigated area mapping.

3.3 *Class identification and labelling*

A comprehensive set of protocols for identifying and labelling the classes was adopted (figure 2(*b*)). Once the classes are grouped by SMTs, each class in a group is investigated by using multiple data sets and the procedures described below, which lead to labelling a class or group of classes.

3.4 *Groundtruth data application*

Precise knowledge of the real situation on the ground is essential to interpret all remote sensing products for the purposes of training, class identification, naming and accuracy assessment. The GIAM project relied on two large groundtruth data sets. These are made available through IWMI data storehouse pathway or

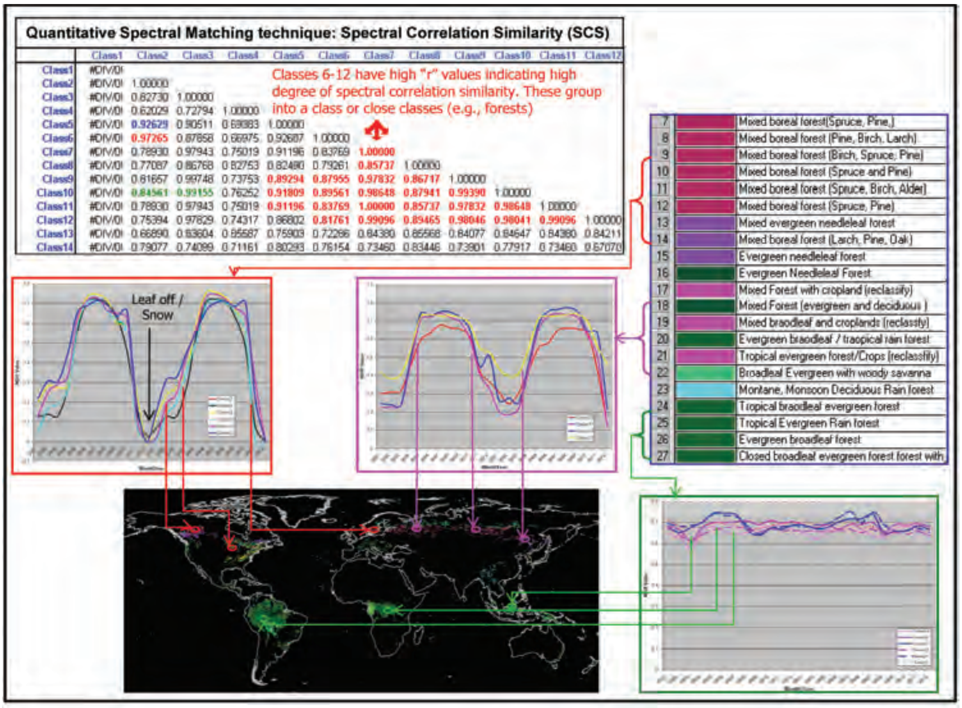

(a)

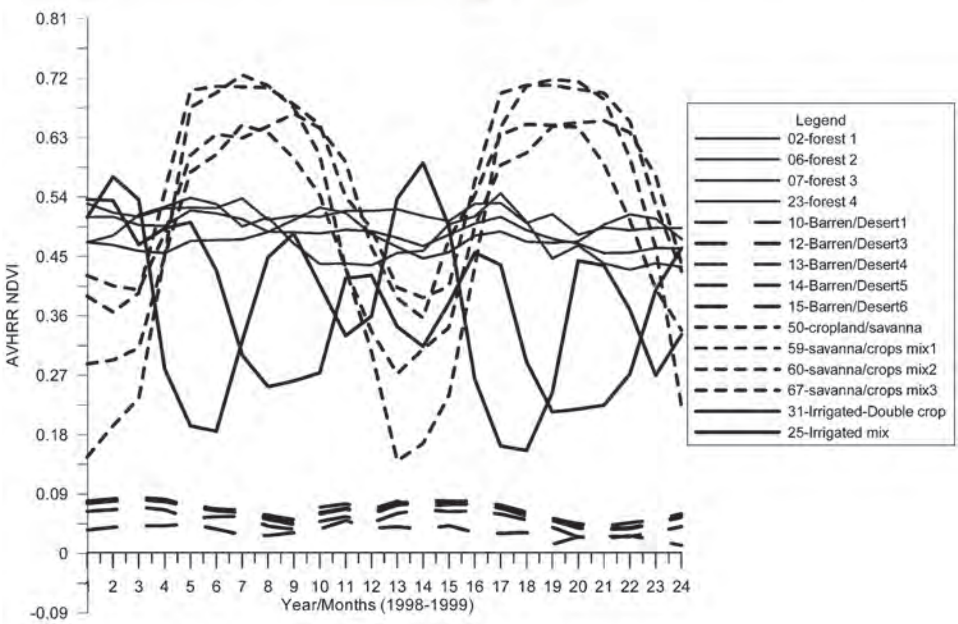

(b)

Figure 3. Spectral Matching Techniques (SMTs) to group classes. The spectral characteristics (e.g. NDVI or spectral reflectivity over time) of any given class is compared with other classes and/or with ideal spectra: (*a*) quantitatively or (*b*) qualitatively.

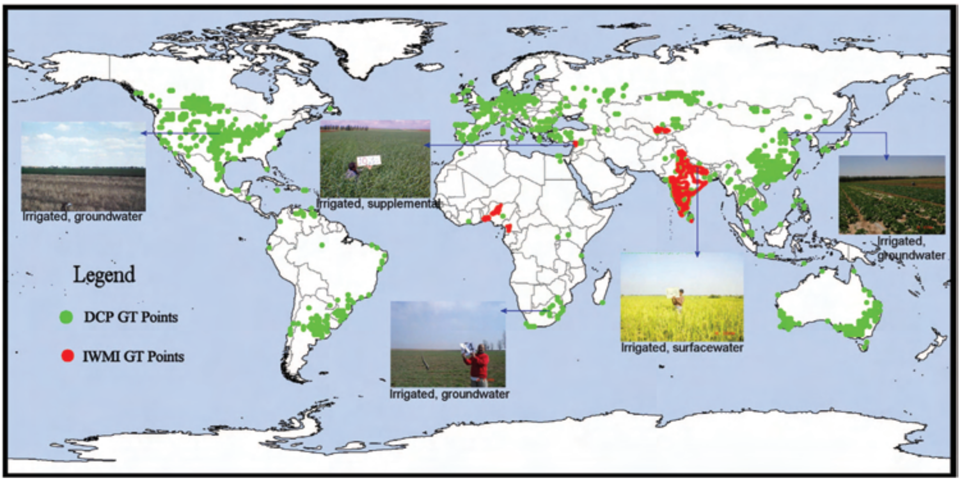

Figure 4. Groundtruth (GT) data for class identification and labelling. Nearly 6 000 groundtruth points were used in the class identification and labelling process. These included 4000+ points from the degree confluence project and nearly 2000 points from the groundtruth missions of the GIAM project.

IWMIDSP (http://www.iwmidsp.org) in standard geographic information system (GIS) formats and are now briefly described.

3.4.1 Public domain groundtruth from the Degree Confluence Project (DCP). The DCP (http://www.confluence.org/) is an organized sampling of the entire world at every 1° latitude and 1° longitude intersection. This is a perfect stratified random sampling, stratified by latitude and longitude grids. It is a voluntary effort. In all, we used 3864 confluence points based on the availability during the project period. The data consisted of precise latitude, longitude, a digital photo of land cover and a description of the land use/land cover (LULC). These were converted to proprietary GIS formats (figure 4) and used in the GIAM class identification and labelling, as well as accuracy assessment along with groundtruth data collected during this project and various VHRI from Google Earth. One in four points (966 points) was used for accuracy assessment. While performing accuracy, the 966 DCP points were added to 1005 points of the GIAM groundtruth data for a total of 1971 points.

3.4.2 Groundtruth data collected by the GIAM team members. Detailed ground truth data were collected by IWMI specifically for the GIAM project similar to procedures and approaches described by Thenkabail *et al.* (2005, 2007a) and Biggs *et al.* (2006). The precise locations of the samples were recorded by GPS in the Universal Transverse Mercator (UTM) and the latitude/longitude coordinate system with a common datum of WGS84. At each location, land use, land cover, crop dominance, crop types, crop growth stages, irrigation source and irrigation intensity were recorded (e.g. figure 4). The statistical design was based on stratified random sampling. They were stratified by the road network, and randomized by the distance from road intersections or time. For example, the sample site locations were selected at 5 km from a road intersection or 5 minute travel from a road intersection. As far as possible, minor road were used. In addition, sampling was carried out using the diversions in these minor roads and travelling a set distance or time from an intersection. In all, 1790 groundtruth points were sourced from India, Sri Lanka, Syria, west and central Africa, South Africa and central Asia. One in two points (895 points) were used in class identification and labelling, and the rest of the 895 points were used in accuracy assessment. An additional 110 points from our very recent missions to the USA, China and Uzbekistan were added to accuracy assessment, making the total points 1005.

3.5 *Utilizing the Google Earth data set for labelling GIAM classes*

Google Earth (http://earth.google.com/) contains increasingly comprehensive image coverage of the globe at very high resolution, 0.61–4m, allowing the user to zoom-in to specific areas in great detail, from a base of 30 m resolution data, based on Geocover 2000. In GIAM, Google Earth data were used for:

- identification and labelling the GIAM classes;
- deriving irrigated area fractions (IAFs) that helped in sub-pixel area (SPA) calculations; and
- assessing accuracy of irrigated area classes.

In all, nearly 11 000+ Google Earth locations were used during the class identification and labelling process (e.g. figure 5). The process starts with zooming in to a precise location and investigating the areas in and around the location. Often, a few thousand hectares are viewed at sub-metre to 4 m by zooming in and around the location, leading to a class name. In order to identify a class, a minimum of 30–60

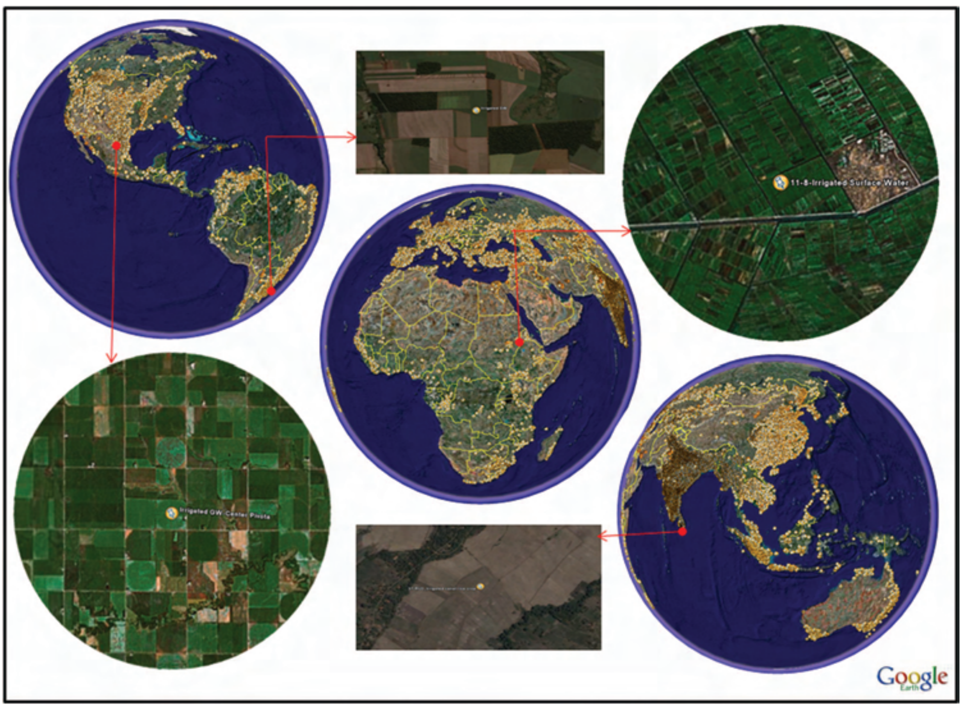

Figure 5. Google Earth data for class identification and labelling. Over 11 000 Google Earth data very-high-resolution imagery (VHRI) 'zoom-in points' were used in class identification and labelling.

spatially well spread out Google Earth data locations were used. The same process is repeated for identifying another class. At the end of the project, in order to identify thousands of classes, 11 000+ Google Earth locations had accumulated. The very-high-resolution data had some real advantage over groundtruth in that they provided information on a much larger area and are, therefore, more representative of the area than is normally sampled directly on the ground. The interpretation of a class is based on visual indicators such as shape (e.g. central pivot circles), size (e.g. large- and small-scale reservoir size), pattern (e.g. contiguous farms) and texture (e.g. the smooth texture of a farm compared to the rough texture of a forest). The date of the 0.61–4 m imagery varies from place to place in Google Earth. Therefore, we may see irrigated area as cropped or fallow depending on the season. Further, Google Earth does not have a wall-to-wall coverage of the 0.61–4 m imagery of the world. In contrast, Geocover has a wall-to-wall coverage at 30 m.

3.6 *Using the Environmental System Research Institute (ESRI) Landsat 150 m Geocover in classification*

The ESRI resampled the 8500 ortho-rectified Landsat ETM+ 30 m 'Geocover' tiles (University of Maryland, http://glcf.umiacs.umd.edu/index.shtml, Tucker *et al.* 2005), and made them available as a single mosaic of the world. These data are used to provide contextual information and pseudo 'groundtruth' by geo-linking to the class maps in order to identify and label classes. The resampled 'Geocover' images have a pixel resolution of 150 m compared with the original pan-sharpened size of 15 m, but provide rapid assessment for checking a class for any part of the world and are positionally the most accurate image set covering the entire globe. The images are optimized to provide maximum greenness for the nominal year 2000, offer a detailed 'zoom-in' view of any part of the world and are ideal for geo-linking to identify and label a class.

The 'zoom-in views' of high-resolution imagery of Geocover 150 m and Google Earth help in class identification in many ways. First, no irrigated classes, such as forests, deserts, water and rangelands, are quickly separated from agricultural lands. Second, irrigation sources, such as central pivot systems and canals, are easily detected (e.g. figure 5). Third, a large number of water bodies in the area implies, but not necessarily confirms, irrigation. In such cases, we will use other data such as groundtruth and knowledge bases of data gathered from the national system (CBIP 1994) to supplement/complement inferences drawn from higher resolution imagery. True cover type is determined based on majority view within the GIAM team on what the class could be in higher resolution imagery similar to interpretative techniques described for the International Geosphere Biosphere Programme (IGBP) DISCover data (see Belward *et al.* 1999, Loveland *et al.* 2000).

3.7 *Techniques for class identification: Space–time spiral curves (ST-SCs) and brightness–greenness–wetness (BGW) plots*

A two-dimensional (2D) near-infrared versus red band spectral reflectivity plot of unsupervised classes is referred to as a BGW plot (Kauth and Thomas 1976, Thenkabail *et al.* 2005). The BGW plots help determine whether a class is: (a) green, (b) bright, (c) wet or (d) somewhere in between these classes. Classes that occupy the green area have high near-infrared reflectivity and low red reflectivity. Typically, these areas are forests, agricultural lands and natural vegetation. Classes that occupy

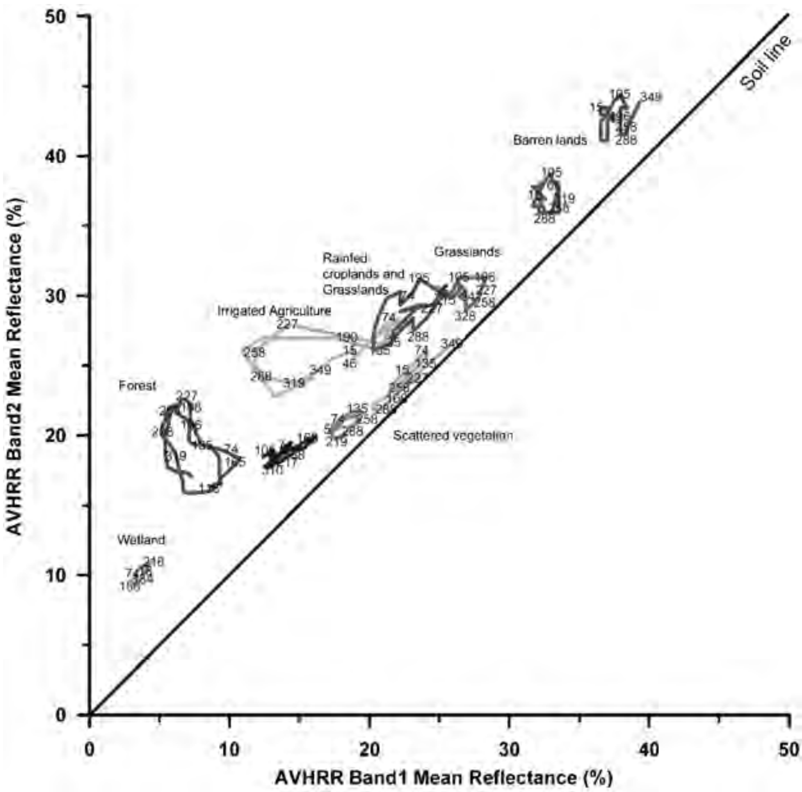

Figure 6. Space–time spiral curves (ST-SCs) in class identification and labelling. The ST-SCs track changes of time series over time and across space. The numbers seen in each class represent Julian date and each class moves around a 'territory' in 2D feature space over time.

bright areas have high near-infrared and high red reflectivity. The LULC categories of these classes are likely to be open/barren areas, sparse vegetation, dry vegetation, clouds and built-up areas. Classes that occupy wet areas have low near-infrared and low red reflectivity. These classes are likely to be wetlands, moist lands, water bodies, cloud shadows and swamp forests. The classes that are in between have different combinations of these broad LULC classes. The BGW plots provide clear and useful information on class dynamics over time and are a very helpful tool in identifying and labelling a class.

The 2D ST-SCs (e.g. figure 6) provide very useful information on class behaviour. Each class has its own 'territory' and moves around in its territory year after year. For example, irrigated areas, forests and rain-fed areas have the largest territories (figure 6). In contrast, barren lands, wetlands, scattered vegetation and grasslands have smaller territories. This approach is used to match and group classes that: (a) fall within similar 2D feature space of a ST-SC plot and (b) have characteristic territory that leads to more precise interpretation of the nature of the class (based on sound field knowledge of at least one or more classes in a group). In figure 6, irrigated areas have the largest 'territory'. It is important to know the spatial distribution of the class and groundtruth knowledge to be definitive of the class name. However, the 2D ST-SCs provide very good indications of the classes based on where they occur and their 'territorial' characteristics.

3.8 *Employing NDVI time series and brightness temperature in identification of categories*

The NDVI time series can categorize and identify irrigated area classes into categories such as double crop (e.g. class 31 in figure 3(*b*)), continuous crop and single crop. For example, time series NDVI are plotted, compared and contrasted, resulting in distinct categories. This is illustrated for five distinct classes in figure 3(*b*): (a) forests, (b) barren/desert lands, (c) savannah croplands, (d) irrigated mix and (d) irrigated double crop.

During the class identification process, the AVHRR time series earth 'skin' temperatures (plots not illustrated) were also plotted along with time series NDVI (figure 3). In the tropics, the greater the biomass levels of a crop, the lower the skin temperature and vice versa. The skin temperatures of irrigated crops are low due to crop transpiration and background moisture/wetness. In the northern hemisphere, crops grown in May–October (summer months) exhibit high NDVI and high skin temperatures. In contrast, during November–April (winter) snow and leaf-off conditions, there are low NDVI and low skin temperatures. Thus, the skin temperature time series helps identify LULC classes in different climatic zones of the world and is often complementary and/or supplementary to NDVI time series plots (see a detailed discussion on skin temperature to LULC classes in Thenkabail *et al.* 2007a).

3.9 *Resolving mixed classes and class verification*

In spite of the rigorous class identification process described above, there are often 'mixed' classes. Typically, the unresolved classes were split up into 10 to 50 sub-classes (depending on extent of area and complexity) before applying the decision tree, GIS spatial modelling and contextual groundtruthing process. Decision tree algorithms (DeFries *et al.* 1998) involving factors such as NDVI, band reflectivity and thermal temperatures in resolving the mixed classes based on the rule base, are followed by class identification and labelling process discussed above. When classes continue to be mixed, in spite of the various methods and techniques discussed in previous sections, we adopted the GIS spatial modelling approaches to resolve classes. This involved taking a mixed class and applying GIS spatial modelling techniques, such as overlay, matrix, recode and sieve and proximity analysis (Leica 2007), based on the theory of map algebra and Boolean logic (Peuquet and Marble 1990, Tomlin 1990, Tomlinson 2003). The GIS spatial data layers used include precipitation zone, elevation zones, Koppen ecological zone, temperature zone and tree cover categories (see figure 2(*b*)). Any one, or a combination of these data layers, often helped separate the mixed classes. Other global LULC products, such as the USGS LULC (Loveland *et al.* 2000, Agrawal *et al.* 2004), USGS seasonal LULC (Loveland *et al.* 2000), GLC2000 (Bartholome and Belward 2005), IGBP (IGBP 1990) and Olson eco-regions of the world (Olson 1994a,b) were also used in verifying final class names assigned in GIAM as a cross check and were specifically useful for verifying no irrigated classes.

3.10 *Class naming convention and the generic map*

The classification of the various segments, identifying and labelling these classes, reclassification of numerous mixed classes and identifying these reclassified classes lead to thousands of classes. Synthesizing these classes becomes extremely complex, unless a standardized system is adopted. In order to make the process seamless and logical for analysts working in the project, we adopted a standard class-naming convention (figure 7), which was supported by groundtruth data, Google Earth data, the SMT and other techniques. This ensured a consistent class-naming pattern irrespective of the analyst. Therefore, every analyst named the classes in a set pattern (see figure 7): watering method, type of irrigation, crop type, scale, intensity, location and type of signature. The irrigation intensity is determined directly using the class signature (e.g. figure 3).

The classes can then be grouped and aggregated as follows:

1.1 Major and medium irrigated areas	1.11 Surface water	1.111 reservoirs with >2000 ha water spread area
2.1 Minor irrigated areas	2.11 Groundwater	2.111 groundwater 2.112 small reservoirs (<2000 ha water spread area) 2.113 Tanks
	2.21 Conjunctive use (surface + groundwater)	
	2.31 Supplemental (predominantly rain-fed with significant irrigation)	

Note. Irrigation by drip, sprinkler, etc. can be from surface water and/or groundwater.

3.11 *Irrigated area estimation through SPA calculations*

The precise irrigated areas are calculated as:

$$\mathrm{SPA}_n = (\mathrm{FPA}_n) \times (\mathrm{IAF}_n), \tag{1}$$

where SPA_n is the SPA of class n; FPA_n is the full-pixel area (FPA) of class n; IAF_n is the irrigated area fraction (IAF) for class n. The FPA is calculated for the 28 GIAM

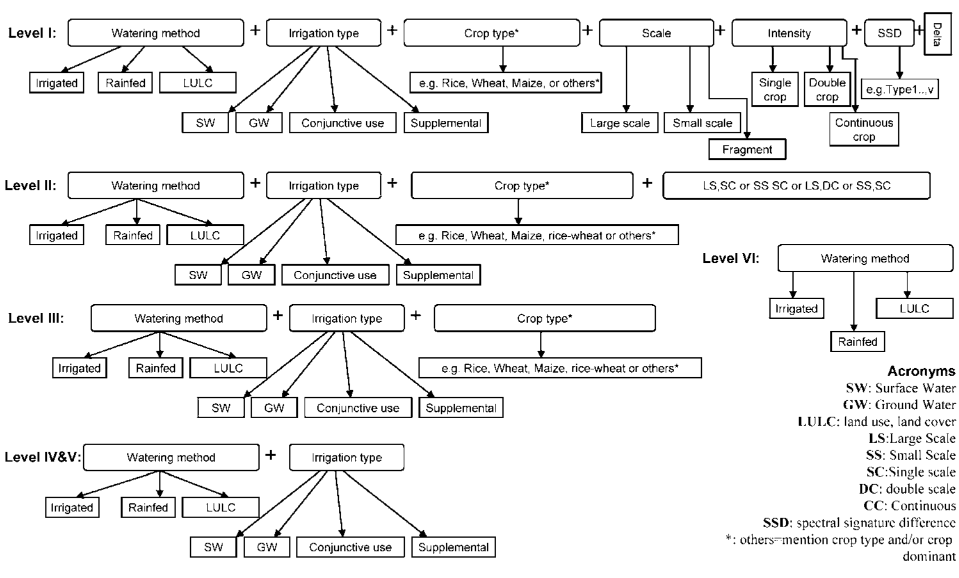

Figure 7. Class labelling protocol. The class labelling protocol 'forces' an analyst to label a class exactly in a standardized pattern so that every analyst labels the class exactly the same way. Shown here are different levels of class labelling.

classes based on Lambert azimuthal equal area (LAEA) projection. The IAFs are determined using the three methods (Thenkabail *et al.* 2007b): (a) Google Earth Estimate (IAF–GEE); (b) high-resolution imagery (IAF–HRI); and (c) sub-pixel decomposition technique (IAF–SPDT).

The reader is referred to Thenkabail *et al.* (2007b) for a detailed understanding of the SPA calculation methods and the IAFs used in this paper.

3.12 *Definition of irrigated areas*

Then two types of irrigated areas were defined and calculated:

(1) TAAI. The TAAI does not consider seasonality or intensity of irrigation. This is the area actually irrigated at any given point of time plus area 'equipped for irrigation', but left fallow at the same point of time. The TAAI is similar to FAO/UF's 'equipped' area and 'net irrigated areas (NIA)' in national statistics. The TAAI is determined by multiplying the FPA by the IAF of the TAAI (IAF_{TAAI}). The IAF_{TAAI} were taken as average of the IAF–GEE and IAF–HRI (of the June–October season) (see IAF_{TAAI} in table 2).
(2) AIA. The AIA considers the seasonality or intensity of irrigation. This is the sum of the areas irrigated during season one and season two, and those that were irrigated continuously throughout the year. The equivalent of AIA in the national statistics is 'gross irrigated area (GIA)'. The AIA is determined by multiplying the FPA by the IAF of the AIA for each season, as well as year round, and then summing up these areas. The IAF_{AIA} were taken as an average of the IAF–HRI and IAF–SPDT of the particular seasons (sea seasonal IAFs in table 2). The seasonality is derived from the AVHRR NDVI profiles of the classes. Each class is observed for single crop (single NDVI peak), double crop (double NDVI peak) and continuous perennial crops, such as plantations (NDVI threshold of 0.4 or more throughout the year). For further details of the cropping calendars, seasons and NDVI profiles, refer to Thenkabail *et al.* (2006) and the GIAM web portal (http://www.iwmigiam.org).

The IAFs of each class for TAAI and AIA are provided in table 2. The TAAI and AIAs are computed by multiplying the respective IAFs with the FPAs.

3.13 *Accuracy assessment*

Accuracies were determined based on two independent data sets. These were:

(1) Accuracy based on groundtruth data from the GIAM project and the DCP. Altogether, 1971 points (966 DCP points plus 1005 GIAM project collected points) were pooled to determine accuracy. Of the 1971 points, 1005 points were irrigated: 463 by surface water and 542 by groundwater. The rest were other LULC and were not used in the final accuracy assessment.
(2) Accuracy based on Google Earth VHRI (sub-metre to 4 m). The groundtruth from Google Earth (GT–GE) generated 670 points that were randomly distributed around the world, with a higher density of distribution of points where the irrigated area is denser. Of the 670 sample points, 323 were irrigated (220 by surface water and 103 by groundwater). The surface-water irrigation was fairly easy to detect with canals, reservoirs and tanks. When there is no evidence of the existence of the surface water, but if the area is

Table 2. Global irrigated areas. The irrigated areas of each of the 28 classes for the world determined by multiplying the full pixel area (FPA) with irrigated area fractions (IAFs) leading to sub-pixel areas (SPAs). The SPAs are actual areas. The annualized irrigated areas (AIAs) is sum of the irrigated areas during season one, season two, and continuous year round. The total area available for irrigation (TAAI) is the irrigated area during any given point of time in the season (taken for the main crop growing season in the world which is during June-October) plus the areas equipped for irrigation but left fallow at the same point of time.

Class Number	Class Names	Full Pixel area (FPA)	Irrigated area fraction (IAF)	Total area available for irrigation or net area	IAF-season1	Season 1 area	IAF-Season 2	Season 2 area	IAF-continuous season	continuous season area	Annualized irrigated areas (AIAs) or gross areas
		hectares	unit less	hectares	unit less	hectares	unit less	hectares	unit less		hectares
1	Irrigated, surface water, single crop, wheat-corn-cotton	10,639,378	0.73	7,766,444	0.61	6,471,843					6,471,843
2	Irrigated, surface water, single crop, cotton-rice-wheat	6,896,128	0.85	5,880,717	0.55	3,813,841					3,813,841
3	Irrigated, surface water, single crop, mixed-crops	14,135,930	0.68	9,628,687	0.46	6,511,261					6,511,261
4	Irrigated, surface water, double crop, rice-wheat-cotton	69,830,220	0.71	49,710,095	0.53	36,711,650	0.67	46,745,513			83,457,163
5	Irrigated, surface water, double crop, rice-wheat-cotton-corn	72,501,012	0.63	45,369,799	0.56	40,938,905	0.52	37,483,023			78,421,928
6	Irrigated, surface water, double crop, rice-wheat-plantations	51,769,022	0.72	37,389,472	0.58	29,807,112	0.48	24,769,631			54,576,742
7	Irrigated, surface water, double crop, sugarcane	2,569,367	0.74	1,910,007	0.67	1,716,980	0.53	1,372,877			3,089,857

Table 2. (*Continued.*)

Class Number	Class Names	Full Pixel area (FPA)	Irrigated area fraction (IAF)	Total area available for irrigation or net area	IAF-season1	Season 1 area	IAF-Season 2	Season 2 area	IAF-continuous season	continuous season area	Annualized irrigated areas (AIAs) or gross areas
8	Irrigated, surface water, double crop, mixed-crops	60,312,587	0.64	38,779,483	0.37	22,446,718	0.37	22,213,443			44,660,161
9	Irrigated, surface water, continuous crop, sugarcane	116,418	0.49	56,932					0.42	49,302	49,302
10	Irrigated, surface water, continuous crop, plantations	13,427,918	0.61	8,184,907					0.44	5,865,373	5,865,373
11	Irrigated, ground water, single crop, rice-sugarcane	12,780,583	0.52	6,653,732	0.49	6,255,930					6,255,930
12	Irrigated, ground water, single crop, corn-soybean	5,997,678	0.70	4,181,556	0.49	2,916,140					2,916,140
13	Irrigated, ground water, single crop, rice and other crops	1,570,188	0.68	1,063,691	0.15	241,540					241,540
14	Irrigated, ground water, single crop, mixed-crops	11,799,752	0.47	5,590,581	0.38	4,518,047					4,518,047
15	Irrigated, ground water, double crop, rice and other crops	3,554,656	0.73	2,583,423	0.55	1,949,455	0.51	1,800,169			3,749,623

Table 2. (*Continued.*)

Class Number	Class Names	Full Pixel area (FPA)	Irrigated area fraction (IAF)	Total area available for irrigation or net area	IAF-season1	Season 1 area	IAF-Season 2	Season 2 area	IAF-continuous season	continuous season area	Annualized irrigated areas (AIAs) or gross areas
16	Irrigated, conjunctive use, single crop, wheat-corn-soybean-rice	29,919,283	0.84	25,082,625	0.47	13,994,126					13,994,126
17	Irrigated, conjunctive use, single crop, wheat-corn-orchards-rice	10,479,639	0.68	7,135,193	0.57	5,982,487					5,982,487
18	Irrigated, conjunctive use, single crop, corn-soybeans-other crops	17,658,270	0.73	12,810,184	0.51	9,039,700					9,039,700
19	Irrigated, conjunctive use, single crop, pastures	9,150,534	0.62	5,672,425	0.25	2,287,634					2,287,634
20	Irrigated, conjunctive use, single crop, pasture, wheat, sugarcane	2,521,549	0.77	1,942,683	0.46	1,162,908					1,162,908
21	Irrigated, conjunctive use, single crop, mixed-crops	17,131,259	0.77	13,120,827	0.57	9,836,226					9,836,226
22	Irrigated, conjunctive use, double crop, rice-wheat-sugarcane	71,510,203	0.67	48,004,873	0.49	35,361,814	0.43	30,967,596			66,329,410
23	Irrigated, conjunctive use, double crop, sugarcane-other crops	1,838,672	0.69	1,265,539	0.39	720,494	0.50	916,272			1,636,766

Table 2. (*Continued.*)

Class Number	Class Names	Full Pixel area (FPA)	Irrigated area fraction (IAF)	Total area available for irrigation or net area	IAF-season1	Season 1 area	IAF-Season 2	Season 2 area	IAF-continuous season	continuous season area	Annualized irrigated areas (AIAs) or gross areas
24	Irrigated, conjunctive use, double crop, mixed-crops	25,756,897	0.51	13,057,718	0.48	12,463,458	0.34	8,700,640			21,164,097
25	Irrigated, conjunctive use, continuous crop, rice-wheat	13,969,654	0.51	7,186,641					0.47	6,618,040	6,618,040
26	Irrigated, conjunctive use, continuous crop, rice-wheat-corn	15,427,976	0.69	10,573,933					0.50	7,672,155	7,672,155
27	Irrigated, conjunctive use, continuous crop, sugarcane-orchards-rice	13,018,909	0.76	9,912,989					0.55	7,168,857	7,168,857
28	Irrigated, conjunctive use, continuous crop, mixed-crops	22,304,422	0.81	18,011,795					0.56	12,393,114	12,393,114

cultivated, then this area becomes a candidate point for rain-fed or groundwater irrigated. This is when the evapo-transpiration (ET) 16 km grid data from the World Water and Climate Atlas (http://www.iwmi.cgiar.org/WAtlas/atlas.htm) was used to determine whether the ET far exceeds precipitation (40 year CRU precipitation data available in http://www.iwmidsp.org). If the answer to this is yes, then irrigation should exist for crops to grow. If the answer to this is no, then the area ought to be rain-fed.

The accuracies were performed to determine how well the irrigated area was mapped. Point-based accuracy and error estimates (Congalton 1994, Foody 2002) were established based on:

$$\text{accuracy of irrigated area class} = \frac{\text{groundtruthed irrigated points classified as irrigated area}}{\text{total number of groundtruthed points for irrigated area class}} \times 100, \quad (2)$$

$$\text{errors of commission for irrigated area classes} = \frac{\text{non-irrigated groundtruth points falling on irrigated area class}}{\text{total number of non-irrigated groundtruthed points}} \times 100, \quad (3)$$

and

$$\text{errors of omission for irrigated area class} = \frac{\text{irrigated groundtruth points falling on non-irrigated area class}}{\text{total number of irrigated area groundtruth points}} \times 100. \quad (4)$$

4. Results

The comprehensive methodology leads to identification and labelling of a final set of classes from each of the seven segments. By aggregating similar types of irrigated area classes, a 28 class global irrigated area map (GIAM28) was produced (figure 8(*a*)), and the area statistics computed for the classes (table 2), continents (table 3) and countries (table 4).

In GIAM28, classes 1–10 are surface water (major and medium irrigation from surface water based on large and medium dams); classes 11–15 are groundwater (minor irrigation from groundwater, small reservoirs and tanks); and classes 16–28 are conjunctive use (predominately minor irrigation from groundwater, small reservoirs and tanks, but with some mix of surface water irrigation from major reservoirs). Within each irrigation type (surface water, groundwater and conjunctive use), there are classes for single, double and continuous cropping (figure 8(*a*) and table 2). Dominant crop types have also been labelled. The GIAM demonstrates the spatial distribution of irrigated areas in the world, and clearly establishes its overwhelming concentration in a few countries such as China, India, the USA and Pakistan (figure 8(*a*)). The presence of a large number of classes in GIAM 28 classes ensures varying seasonality of classes by taking more precise cropping calendars between northern and southern hemispheres, the tropics and the higher latitudes.

(*a*)

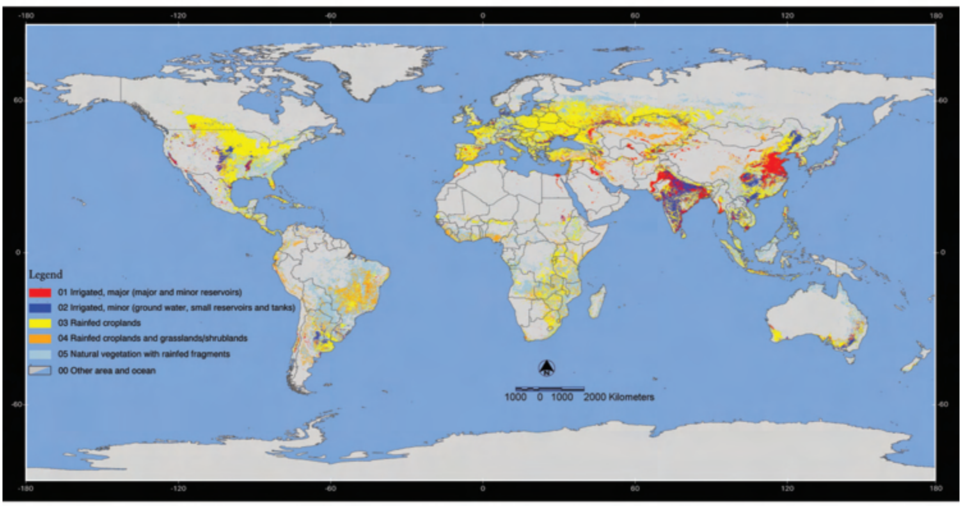

(*b*)

Figure 8. Global Irrigated Area Maps (GIAMs). (*a*) The aggregated 28 class GIAM product and (*b*) the irrigated croplands of the world along with the rain-fed croplands of the world.

The distribution of the irrigated areas (figure 8(*a*)) are overlaid on rain-fed cropland areas of a parallel study (Biradar *et al.* 2009, http://www.iwmigiam.org) using the same methodology. This shows the spatial distribution of irrigated croplands relative to rain-fed croplands of the world (figure 8(*b*)). China and India with about 2.4 billion people depend on irrigation and often have double cropping to feed their populations. In contrast, North America and Europe, with a combined population of about 1.3 billion, depend on rain-fed agriculture (figure 8(*b*)), with only one crop per year. They also export large quantities of their food grains to other countries and continents. Throughout this paper, we discuss the global irrigated areas (figure 8(*a*) and table 2). The global rain-fed croplands (Biradar *et al.* 2009) distribution overlaid on the global irrigated areas (figure 8(*b*)) is presented briefly for

Table 3. Continental irrigated areas based on GIAM. The distribution of irrigated areas and their percentages in different continents of the world.

	Continent	SPA_{TAAI} [1] (TAAI) (ha)	SPA–HRI/SPDT: IWMI GIAM 10 km V2.0 (actual irrigated area)[2] Season 1 (ha)	Season 2 (ha)	Continuous (ha)	Annualized sum (ha)	Percentage of world total (%)	FAO/UF V4.0[3] (Area equipped for Irrigation) (ha)
1	Africa	8 687 044	5 601 273	3 680 659	1 020 078	10 302 011	2	13 432 285
2	Asia	290 641 673	192 600 664	152 312 096	24 700 163	369 612 923	79	187 600 089
3	Australia	11 865 244	2 991 344	0	2 382 064	5 373 409	1	2 056 580
4	Europe	33 937 745	20 126 797	7 691 113	4 627 243	32 445 154	7	26 770 001
5	North America	35 426 895	22 316 537	6 448 147	3 089 990	31 854 673	7	36 889 071
6	South America	17 842 959	8 055 356	3 363 798	5 608 671	17 027 825	4	11 495 806
7	Oceania	125 390	68 146	58 034	15 505	141 686	0	581 254
	TOTAL	398 526 951	251 760 118	173 553 847	41 443 716	466 757 680	100	278 825 086

Note. (1) SPA from combined coefficients of Google Earth estimate and high-resolution images, (2) SPA from combined coefficients of high-resolution images and sub-pixel decomposition technique, (3) area irrigated obtained from FAO AQUASTAT and Earth trends (http://www.fao.org/ag/agl/aglw/aquastat/water_use/croppat.htm/ http://earthtrends.wri.org/country_profiles/index.php?theme=8).

Table 4. Country-by-country irrigated areas based on GIAM. The distribution of irrigated areas and their percentages for the 198 countries in the world and their comparison with the FAO AQUASTAT, which is based on the country statistics.

Rank	Country	SPA_{TAAI}[1] (TAAI) (ha)	SPA–HRI/SPDT: IWMI GIAM 10 km V2.0 (actual irrigated area)[2] Season 1 (ha)	Season 2 (ha)	Continuous (ha)	Annualized (ha)	Irrigated area (%)	FAO/UF V4.0[3] (area equipped for irrigation) (ha)
1	China	111 988 772	75 880 320	68 233 355	7 688 411	151 802 086	32.523	53 823 000
2	India	101 234 893	72 612 189	53 685 066	5 956 598	132 253 854	28.335	57 291 407
3	USA	28 045 478	18 182 104	4 006 141	2 120 942	24 309 188	5.208	27 913 872
4	Pakistan	14 036 151	7 895 566	7 302 243	761 533	15 959 342	3.419	14 417 464
5	Russia	13 886 856	8 865 013	2 113 783	224 734	11 203 530	2.400	4 899 900
6	Argentina	9 304 258	3 601 505	1 605 815	3 559 092	8 766 412	1.878	1 767 784
7	Thailand	6 610 586	3 228 550	2 209 523	1 959 295	7 397 368	1.585	4 985 708
8	Bangladesh	5 235 050	3 882 847	3 076 494	206 686	7 166 028	1.535	3 751 045
9	Kazakhstan	7 227 718	4 625 716	1 760 606	83 362	6 469 685	1.386	1 855 200
10	Myanmar(Burma)	4 452 997	3 360 330	2 798 234	148 108	6 306 671	1.351	1 841 320
11	Australia	11 865 244	2 991 344	0	2 382 064	5 373 409	1.151	2 056 580
12	Uzbekistan	3 601 487	2 733 397	2 427 259	134 859	5 295 515	1.135	4 223 000
13	Vietnam	4 384 022	1 865 074	1 419 401	1 665 058	4 949 533	1.060	3 000 000
14	Brazil	4 195 118	2 165 151	869 365	1 051 327	4 085 844	0.875	3 149 217
15	Mexico	3 854 673	1 818 168	916 083	874 479	3 608 730	0.773	6 435 800
16	Indonesia	3 172 879	1 221 384	716 038	1 385 021	3 322 443	0.712	4 459 000
17	Egypt	2 144 099	1 635 323	1 491 605	165 798	3 292 726	0.705	3 422 178
18	Spain	3 421 724	1 516 815	683 698	825 310	3 025 823	0.648	3 575 488
19	Germany	2 197 697	1 642 692	1 318 567	40 415	3 001 674	0.643	496 871
20	Canada	2 658 297	1 727 915	1 124 721	21 616	2 874 252	0.616	785 046
21	France	2 399 518	1 249 368	829 980	607 806	2 687 153	0.576	2 906 081
22	Italy	2 829 523	1 342 442	539 802	761 896	2 644 140	0.566	3 892 202
23	Iraq	2 220 024	1 242 694	1 254 929	128 942	2 626 564	0.563	3 525 000
24	Iran	2 623 336	1 308 727	679 564	500 268	2 488 558	0.533	6 913 800
25	Japan	2 525 096	1 157 850	656 470	654 276	2 468 596	0.529	3 129 000
26	Ukraine	2 995 578	1 631 677	258 515	491 607	2 381 799	0.510	2 395 500
27	Korea, Dem. Rep.	1 467 262	935 934	923 533	194 157	2 053 625	0.440	1 460 000
28	Romania	2 375 239	1 128 692	315 485	605 711	2 049 888	0.439	2 149 903
29	Turkmenistan	1 522 372	994 264	904 352	101 368	1 999 984	0.428	1 744 100

Table 4. (*Continued.*)

Rank	Country	SPA_{TAAI}[1] (TAAI) (ha)	SPA–HRI/SPDT: IWMI GIAM 10 km V2.0 (actual irrigated area)[2]				Irrigated area (%)	FAO/UF V4.0[3] (area equipped for irrigation) (ha)
			Season 1 (ha)	Season 2 (ha)	Continuous (ha)	Annualized (ha)		
30	Sudan	1 737 118	1 185 252	643 655	101 685	1 930 592	0.414	1 863 000
31	Philippines	1 542 629	1 024 930	589 003	175 175	1 789 108	0.383	1 550 000
32	Turkey	1 753 382	882 867	332 404	362 042	1 577 313	0.338	4 185 910
33	Nepal	1 251 988	681 267	530 989	265 047	1 477 303	0.317	1 168 349
34	Chile	1 514 922	703 120	345 867	396 243	1 445 230	0.310	1 900 000
35	Korea, Rep.	1 192 469	546 413	432 289	335 053	1 313 755	0.281	880 365
36	Morocco	1 045 119	578 582	460 512	114 723	1 153 817	0.247	1 458 160
37	United Kingdom	970 733	810 688	233 603	15 913	1 060 204	0.227	228 950
38	Bulgaria	1 301 804	579 629	62 782	369 652	1 012 064	0.217	545 160
39	Netherlands	870 243	681 847	299 991	29 502	1 011 340	0.217	476 315
40	Denmark	1 164 705	976 705	2 835	0	979 539	0.210	476 000
41	Cambodia	736 318	480 153	329 683	128 606	938 441	0.201	284 172
42	Afghanistan	1 008 138	403 083	218 706	301 701	923 490	0.198	3 199 070
43	South Africa	821 040	574 487	206 929	47 075	828 491	0.177	1 498 000
44	Azerbaijan	835 627	441 335	218 092	162 553	821 980	0.176	1 453 318
45	Sri Lanka	948 029	169 255	111 161	529 164	809 579	0.173	570 000
46	Venezuela	894 880	499 284	93 686	214 109	807 078	0.173	570 219
47	Kyrgyzstan	700 876	447 852	247 134	75 288	770 274	0.165	1 075 040
48	Greece	907 739	271 632	106 151	388 895	766 678	0.164	1 544 530
49	Czech Republic	518 036	380 186	321 296	245	701 727	0.150	50 590
50	Taiwan, Province of China	499 043	282 608	314 359	80 910	677 877	0.145	525 528
51	Cuba	486 898	342 202	269 666	25 291	637 159	0.137	870 319
52	Syria	566 990	302 293	235 219	58 751	596 263	0.128	1 266 900
53	Colombia	546 186	336 538	176 558	79 399	592 495	0.127	900 000
54	Saudi Arabia	678 677	143 187	89 073	318 806	551 066	0.118	1 730 767
55	Belgium	324 796	294 221	204 916	8 293	507 430	0.109	35 170
56	Poland	351 514	268 183	185 150	779	454 111	0.097	134 050
57	Tajikistan	383 243	277 736	156 376	15 040	449 153	0.096	719 200
58	Somalia	372 476	162 324	117 817	123 434	403 574	0.086	200 000
59	Mongolia	422 332	265 966	110 413	0	376 378	0.081	57 300

Table 4. (*Continued.*)

Rank	Country	SPA_{TAAI}[1] (TAAI) (ha)	SPA–HRI/SPDT: IWMI GIAM 10 km V2.0 (actual irrigated area)[2]				Irrigated area (%)	FAO/UF V4.0[3] (area equipped for irrigation) (ha)
			Season 1 (ha)	Season 2 (ha)	Continuous (ha)	Annualized (ha)		
60	Peru	355 956	189 766	113 945	71 243	374 954	0.080	1 729 069
61	Uruguay	381 403	311 863	25 602	22 591	360 055	0.077	217 593
62	Guinea	302 633	153 448	95 459	71 442	320 350	0.069	94 914
63	Portugal	358 865	133 115	54 464	126 330	313 908	0.067	792 008
64	Senegal	211 416	148 318	129 202	13 052	290 572	0.062	119 680
65	Ecuador	288 581	127 918	85 157	68 091	281 166	0.060	863 370
66	Malaysia	258 766	123 739	66 638	84 189	274 565	0.059	362 600
67	Serbia	171 939	140 266	92 171	1 910	234 348	0.050	163 311
68	Moldova	294 070	161 373	20 311	47 749	229 433	0.049	307 000
69	Albania	223 777	117 469	55 223	53 172	225 864	0.048	340 000
70	Nigeria	197 909	103 154	61 884	51 115	216 154	0.046	293 117
71	Libya	230 656	67 173	60 076	82 773	210 022	0.045	470 000
72	Hungary	241 714	166 069	14 990	5 162	186 221	0.040	292 147
73	Bolivia	214 091	28 854	9 777	124 404	163 036	0.035	128 240
74	Ethiopia	184 239	62 157	25 604	75 047	162 808	0.035	289 530
75	Guinea Bissau	108 042	84 650	66 770	3 969	155 389	0.033	22 558
76	Georgia	128 538	96 950	46 285	2 907	146 141	0.031	300 000
77	New Zealand	125 390	68 146	58 034	15 505	141 686	0.030	577 882
78	Algeria	144 349	90 667	34 731	11 548	136 946	0.029	569 418
79	Macedonia	169 843	113 105	9 610	8 905	131 620	0.028	127 800
80	Armenia	106 695	73 185	37 092	8 047	118 324	0.025	286 027
81	Laos	105 585	78 350	21 795	7 589	107 734	0.023	295 535
82	Israel	99 806	39 883	37 020	27 639	104 542	0.022	183 408
83	Kenya	85 401	53 025	37 354	14 148	104 527	0.022	103 203
84	Guyana	96 276	61 736	30 935	10 259	102 930	0.022	150 134
85	Cote d'Ivoire	95 138	79 392	20 756	1 742	101 890	0.022	72 750
86	Tunisia	109 144	30 355	23 663	46 628	100 647	0.022	394 063
87	Austria	116 456	69 017	19 025	10 509	98 551	0.021	97 480
88	Swaziland	149 274	97 004	0	0	97 004	0.021	49 860
89	Guatemala	69 373	47 776	40 864	2 673	91 313	0.020	129 803
90	Dominican Republic	70 876	45 462	25 851	8 335	79 648	0.017	269 710

Table 4. (*Continued.*)

Rank	Country	SPA_{TAAI}[1] (TAAI) (ha)	SPA–HRI/SPDT: IWMI GIAM 10 km V2.0 (actual irrigated area)[2]				Irrigated area (%)	FAO/UF V4.0[3] (area equipped for irrigation) (ha)
			Season 1 (ha)	Season 2 (ha)	Continuous (ha)	Annualized (ha)		
91	Yemen	91 688	42 912	16 073	20 203	79 188	0.017	388 000
92	Honduras	70 584	51 034	21 071	5 623	77 729	0.017	73 210
93	Slovakia	109 904	71 826	1 044	2 618	75 488	0.016	15 643
94	Madagascar	72 359	41 627	19 039	14 490	75 156	0.016	1 086 291
95	Finland	125 307	71 961	0	0	71 961	0.015	103 800
96	Ghana	60 647	28 411	24 173	19 181	71 764	0.015	30 900
97	Sweden	83 918	69 968	1 140	0	71 108	0.015	188 470
98	United Arab Emirates	93 810	10 249	4 867	55 487	70 603	0.015	280 341
99	Mali	56 355	38 220	26 100	1 559	65 879	0.014	235 791
100	Rwanda	80 067	64 806	0	0	64 806	0.014	8 500
101	Thegambia	39 872	34 993	28 422	0	63 415	0.014	0
102	Belarus	84 088	60 731	195	0	60 926	0.013	115 000
103	Mozambique	56 415	39 402	16 753	4 587	60 742	0.013	118 120
104	Haiti	50 848	29 974	15 438	8 490	53 903	0.012	91 502
105	Jordan	72 717	574	568	51 399	52 541	0.011	76 912
106	Cameroon	52 694	35 415	5 861	10 852	52 128	0.011	25 654
107	Tanzania	47 022	33 678	7 852	5 467	46 998	0.010	184 330
108	Panama	49 069	21 997	6 477	16 574	45 048	0.010	34 626
109	Croatia	35 202	28 102	15 511	1 018	44 630	0.010	5 790
110	Lithuania	57 272	41 591	0	0	41 591	0.009	4 416
111	Switzerland	29 523	21 079	15 897	0	36 976	0.008	40 000
112	Angola	23 316	16 671	14 371	3 116	34 158	0.007	80 000
113	Uganda	30 017	26 957	3 447	183	30 586	0.007	9 150
114	Oman	17 853	15 247	14 898	0	30 145	0.006	72 630
115	Sierra Leone	21 807	16 343	12 481	213	29 037	0.006	29 360
116	Chad	25 234	15 932	8 020	3 747	27 698	0.006	30 273
117	Qatar	38 509	0	0	27 596	27 596	0.006	12 520
118	Kuwait	37 333	0	0	26 753	26 753	0.006	6 968
119	Lebanon	24 747	11 240	8 170	5 859	25 268	0.005	117 113
120	Paraguay	28 582	12 913	1 670	10 445	25 029	0.005	67 000

Table 4. (*Continued.*)

Rank	Country	SPA_{TAAI}[1] (TAAI) (ha)	SPA–HRI/SPDT: IWMI GIAM 10 km V2.0 (actual irrigated area)[2] Season 1 (ha)	Season 2 (ha)	Continuous (ha)	Annualized (ha)	Irrigated area (%)	FAO/UF V4.0[3] (area equipped for irrigation) (ha)
121	Togo	21 727	9 624	7 433	6 786	23 843	0.005	7 300
122	Nicaragua	16 439	12 165	9 941	614	22 720	0.005	61 365
123	Suriname	19 845	14 491	5 070	1 213	20 774	0.004	51 180
124	Congo, Dem. Rep.	21 833	19 326	191	857	20 375	0.004	10 500
125	Mauritania	15 124	9 814	10 007	214	20 036	0.004	45 012
126	Costa Rica	12 628	9 730	5 448	613	15 791	0.003	103 084
127	Benin	15 173	4 383	3 797	7 235	15 415	0.003	12 258
128	Burkina Faso	15 663	4 539	4 420	5 702	14 660	0.003	25 000
129	Estonia	24 637	14 476	0	0	14 476	0.003	1 363
130	Bosnia and Herzegovina	10 766	6 696	5 445	2 062	14 203	0.003	4 630
131	Montenegro	10 331	6 940	5 604	1 364	13 908	0.003	0
132	Eritrea	17 017	11 467	2 309	0	13 776	0.003	21 590
133	Puerto Rico	11 964	7 082	1 582	2 588	11 253	0.002	37 079
134	El Salvador	11 592	7 839	2 508	54	10 401	0.002	44 993
135	Namibia	10 526	7 508	1 795	0	9 303	0.002	7 573
136	Burundi	11 793	534	36	7 921	8 490	0.002	21 430
137	Latvia	12 683	7 260	65	0	7 325	0.002	1 150
138	Gaza Strip	5 909	3 192	3 223	375	6 790	0.001	0
139	Cyprus	7 099	2 751	129	1 983	4 863	0.001	55 813
140	Jamaica	4 881	3 058	492	1 006	4 556	0.001	25 214
141	Niger	4 129	3 121	1 196	0	4 317	0.001	73 663
142	Botswana	5 417	3 687	590	0	4 278	0.001	1 439
143	East Timor	3 800	3 257	804	0	4 061	0.001	14 000
144	Mauritius	5 312	2 381	0	1 528	3 910	0.001	21 222
145	Lesotho	5 675	3 681	0	0	3 681	0.001	2 638
146	Zimbabwe	4 744	3 234	299	0	3 533	0.001	173 513
147	Belize	3 887	2 919	306	286	3 510	0.001	3 000
148	French Guyana	2 860	2 217	351	254	2 822	0.001	2 000
149	Malawi	3 293	2 794	0	0	2 794	0.001	56 390
150	Equatorial guinea	2 812	2 644	0	0	2 644	0.001	0

Table 4. (*Continued.*)

Rank	Country	SPA_{TAAI}[1] (TAAI) (ha)	SPA–HRI/SPDT: IWMI GIAM 10 km V2.0 (actual irrigated area)[2] Season 1 (ha)	Season 2 (ha)	Continuous (ha)	Annualized (ha)	Irrigated area (%)	FAO/UF V4.0[3] (area equipped for irrigation) (ha)
151	Antigua and Barbuda	2 270	1 378	706	384	2 468	0.001	130
152	Guadeloupe	1 894	1 498	342	183	2 022	0.000	2 000
153	Trinidad and Tobago	1 859	1 672	0	48	1 720	0.000	3 600
154	West Bank	1 612	538	533	471	1 542	0.000	0
155	Norway	2 072	1 323	130	0	1 453	0.000	134 396
156	St. Kitts and Nevis	1 650	1 314	84	48	1 445	0.000	18
157	Bhutan	997	796	600	0	1 396	0.000	38 734
158	Central African Republic	1 155	1 086	0	0	1 086	0.000	135
159	Virgin Islands	827	563	361	91	1 015	0.000	185
160	Brunei	799	481	369	152	1 002	0.000	1 000
161	Reunion	651	517	329	0	846	0.000	13 000
162	San Marino	1 102	0	0	797	797	0.000	0
163	Djibouti	905	587	0	0	587	0.000	1 012
164	Zambia	779	0	0	536	536	0.000	155 912
165	Slovenia	439	293	217	0	510	0.000	0
166	Comoros	241	218	199	0	417	0.000	130
167	Anguilla	489	404	0	0	404	0.000	0
168	Liberia	237	201	100	0	300	0.000	2 100
169	Turks and Caicos Islands	214	117	0	53	170	0.000	0
170	Montserrat	69	51	65	0	115	0.000	0
171	St. Pierre and Miquelon	70	59	0	0	59	0.000	0
172	Cayman Islands	66	55	0	0	55	0.000	0
173	Monaco	73	0	0	53	53	0.000	0
174	Seychelles	66	44	0	0	44	0.000	260
175	Andorra	0	0	0	0	0	0.000	150
176	Bahrain	0	0	0	0	0	0.000	4 060
177	Barbados	0	0	0	0	0	0.000	1 000

Table 4. (*Continued.*)

Rank	Country	SPA_{TAAI}[1] (TAAI) (ha)	SPA–HRI/SPDT: IWMI GIAM 10 km V2.0 (actual irrigated area)[2] Season 1 (ha)	Season 2 (ha)	Continuous (ha)	Annualized (ha)	Irrigated area (%)	FAO/UF V4.0[3] (area equipped for irrigation) (ha)
178	Cape Verde	0	0	0	0	0	0.000	3 109
179	Congo	0	0	0	0	0	0.000	2 000
180	Fiji	0	0	0	0	0	0.000	3 000
181	Gabon	0	0	0	0	0	0.000	4 450
182	Gambia	0	0	0	0	0	0.000	2 149
183	Grenada	0	0	0	0	0	0.000	219
184	Guam	0	0	0	0	0	0.000	312
185	Ireland	0	0	0	0	0	0.000	1 100
186	Liechtenstein	0	0	0	0	0	0.000	0
187	Luxembourg	0	0	0	0	0	0.000	27
188	Malta	0	0	0	0	0	0.000	2 300
189	Martinique	0	0	0	0	0	0.000	3 000
190	Northern Marianna Islands	0	0	0	0	0	0.000	60
191	Palestine	0	0	0	0	0	0.000	19 466
192	Papua New Guinea	0	0	0	0	0	0.000	0
193	Pitcairn Islands	0	0	0	0	0	0.000	0
194	Sao Tome and Principe	0	0	0	0	0	0.000	9 700
195	Singapore	0	0	0	0	0	0.000	225 310
196	St. Lucia	0	0	0	0	0	0.000	297
197	St. Vincent and the Grenadines	0	0	0	0	0	0.000	0
198	Vatican city	0	0	0	0	0	0.000	0
	TOTAL	398 526 951	251 760 118	173 553 847	41 443 716	466 757 680	100.000	278 825 086

Note. (1) SPA from combined coefficients of Google Earth estimate and high-resolution images, (2) SPA from combined coefficients of high-resolution images and sub-pixel decomposition technique, (3) area equipped for irrigation from FAO and UF Global Map of Irrigated Area V3.0 (based on national statistics), (4) area irrigated obtained from FAO AQUASTAT and Earth trends (http://faostat.fao.org/faostat/ http://earthtrends.wri.org/country_profiles/).

discussion purposes and for showing the spatial distribution of the croplands. The results of the rain-fed croplands or other LULC is not the focus of this paper, and further presentation of results and discussions will be overwhelmingly focused on the GIAM.

4.1 *Irrigated areas of the world*

Irrigated areas of the world are calculated with and without considering the intensity or seasonality. The TAAI does not consider intensity and provides area irrigated plus area left fallow at any given point of time. This is equivalent to NIAs. The AIA considers intensity or seasonality. The AIA is the sum of the area irrigated during season one, season two and continuous year-round crops, such as sugarcane, or permanent crops, such as plantations (table 2). The nearest equivalent of the AIA in the national statistics is 'GIA'.

The total AIAs of the world are 467 Mha, of which 252 Mha are during season one, 174 Mha during season two and 41 Mha continuous (figure 8(*a*) and table 2). The TAAI is 399 Mha. Of the AIA of 467 Mha, a high proportion of 55% (267 Mha) is surface-water irrigation with double crop (table 2). Only about 5% of the AIA is surface water, single crop and 1% surface water, continuous crop. The total surface-water irrigation (classes 1–10 in table 2) is, therefore, 61%. The conjunctive use classes (classes 16–28) are overwhelmingly groundwater-dominant with very minor (roughly, less than 15%) surface-water influence. Therefore, if we group all the groundwater classes from 11 to 15 and conjunctive use classes from 16 to 28 into one category, the total groundwater irrigation in the world will be 39% of the AIA (or 186 Mha). Of the 39% groundwater irrigation, 19% were double crop, 12% single crop and 8% continuous cropping. The distribution of irrigated areas in the continents and countries was summarized in tables 3 and 4, respectively.

The FAO of the United Nations and the UF estimates the 'equipped' area for irrigation (but not necessarily irrigated) in the world to be 279 Mha (http://www.fao.org/ag/agl/aglw/aquastat/irrigationmap/index.stm; also reported in http://www.iwmigiam.org, Siebert *et al.* 2005a,b, 2006). Based on the definition, the FAO/UF values (279 Mha) should be compared with GIAM TAAI (399 Mha) (table 4). The reasons for these differences are discussed in §4.6. The GIAM AIA is 467 Mha of which season one (June–October) has 252 Mha, season two (November–February) has 174 Mha and continuous year-round has 41 Mha. An overwhelming proportion of the global agriculture takes place during season one. It is the main cropping season of all major irrigated area countries, including China, India, the USA, Pakistan and most of the Asian and central Asian countries. Together, these countries have over 85% of global irrigation.

4.2 *Global irrigated area trends over the last two centuries*

The development of global irrigated areas over the last two centuries (Framji *et al.* 1981, http://www.iwmigiam.org, http://www.fao.org/ag/agl/aglw/aquastat/irrigationmap/index.stm) is summarized in figure 9. In the year 1800, there was a meagre 8 Mha irrigated area (Framji *et al.* 1981). As the trends in figure 9 show, the increase in irrigated areas for the next 140 years was modest, reaching a value of 95 Mha in the early 1940s (Van Schilfgaarde 1994). Rapid increases in global irrigated areas took place between 1940 and 2000. The FAO/UF global area 'equipped for irrigation' was around 279 Mha by the mid-1990s (see http://www.iwmigiam.org, http://www.fao.org/ag/agl/aglw/aquastat/irrigationmap/index.stm, Döll and Siebert 2000, Siebert *et al.* 2005a,b,

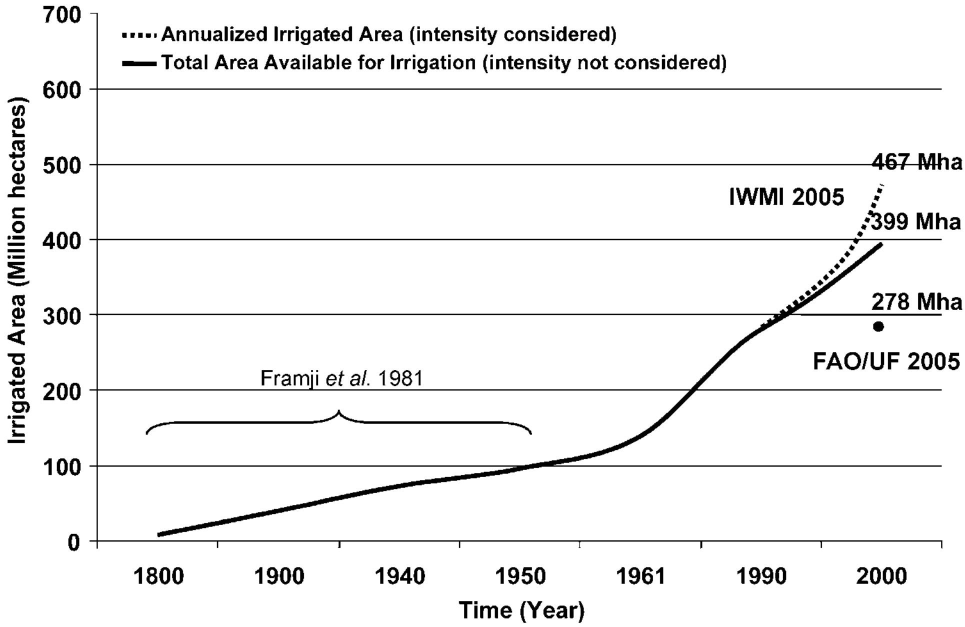

Figure 9. Global irrigated area trends. The global irrigated areas at the end of the last millennium (this study) were provided as: (*a*) annualized irrigated areas (AIAs), which consider cropping intensity or seasonality (sum of irrigated areas during season one + season two + continuous year-round), and (*b*) total area available for irrigation (TAAI), which does not consider intensity and is area irrigated at any given time plus the area equipped for irrigation but remains fallow at the same point of time. In the national statistics, AIA is often referred to as 'gross irrigated area' and TAAI as 'net irrigated area'. The figure also shows the trends of irrigation from year 1800 gathered from various sources.

2006). In this study (figures 9(*a*) and 10 and tables 2, 3 and 4), irrigated areas at the end of the last millennium were reported after: (a) considering intensity (cropped areas from different seasons are added) and (b) without considering intensity (NIA). Considering intensity (i.e. AIA), the irrigated area was 467 Mha. Without considering intensity (i.e. TAAI), it was 399 Mha.

4.3 *Irrigated areas of the continents*

Of the 467 Mha AIAs in the world, Asia accounts for 79% (370 Mha), followed by Europe (7%) and North America (7%) (see table 3). Three continents, South America (4%), Africa (2%) and Australia (1%), have a very low proportion of the global annualized irrigation (table 3). In Europe and North America, an overwhelming proportion of irrigation is during the one main cropping season (May–October). In Asia, 154 Mha are irrigated in season two (November–February) compared with 195 Mha during season one (May–October), showing strong double cropping. In Asia, the TAAI is 291 Mha, so the intensity of cropping is 127% (370/291), compared to the global intensity of 117% (467/399).

4.4 *Irrigated areas of the countries*

Irrigated area statistics are provided for the 198 countries (table 4) and compared with FAO/UF AQUASTATS. The countries have been ranked based on the global

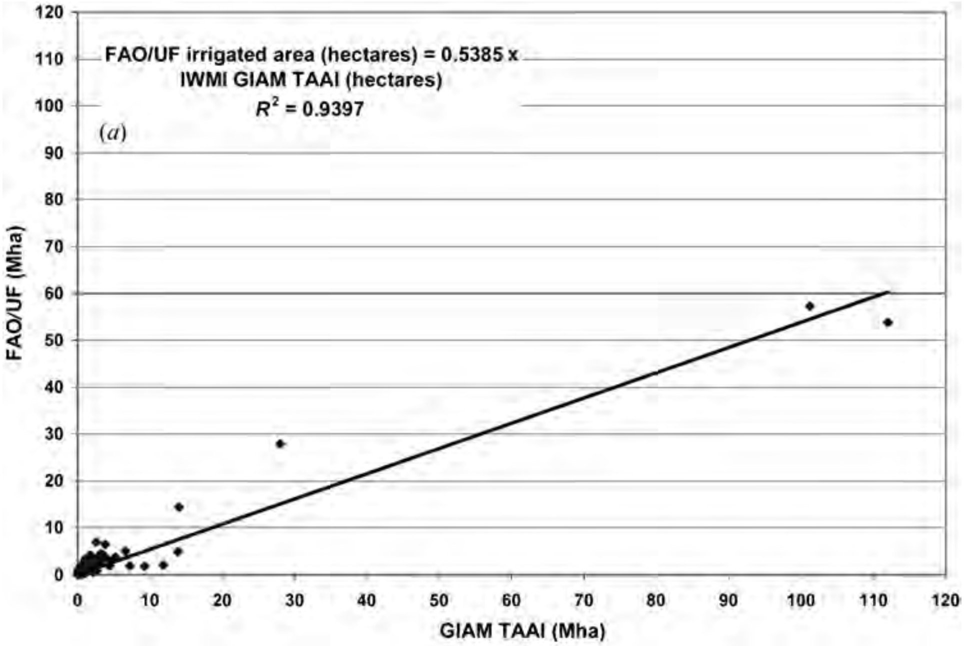

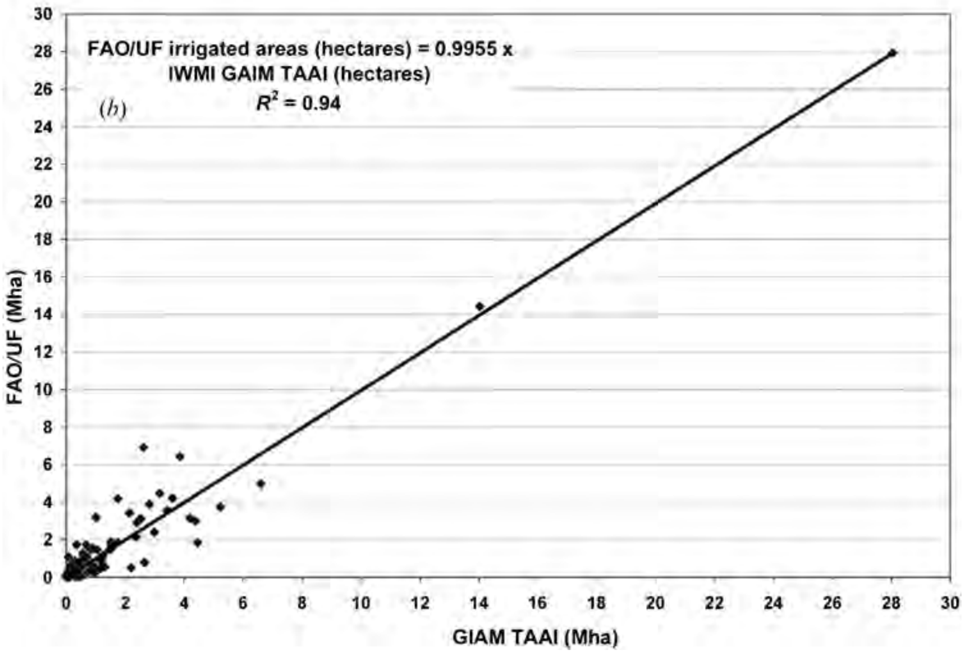

Figure 10. Comparison of GIAM country-by-country irrigated areas with FAO/UF country-by-country irrigated areas. The GIAM areas are correlated with the FAO/UF statistics for: (*a*) all the 198 countries and (*b*) 154 countries leaving out the 37 countries with near-zero areas (either in FAO or GIAM) and seven countries where the two differ by large margins.

AIA. Of the total global AIA of 467 Mha, China has 32.5% and India has 28.3%; together constituting a staggering total of nearly 63%. The next ranked countries have comparatively low percentage AIAs: USA (5.2%), Pakistan (3.4%) and Russia

(2.4%). There are eight countries (Argentina, Thailand, Bangladesh, Kazakhstan, Myanmar, Australia, Uzbekistan and Vietnam) with 1 to 2% irrigation. Brazil is ranked 14th with 0.88%, followed by Mexico, Indonesia and Egypt with around 0.7% each (table 4). All other countries of the world have less than 0.7% each of the global AIA. The first 40 countries, ranked in table 4, have nearly 96% of all AIAs of the world. Most studies (e.g. Postel 1999, Droogers 2002) consider India as the leading irrigated area country, closely followed by China. However, our estimates show that China has 152 Mha of AIA, while India has 132 Mha. In season one (June–October) China with 76 Mha and India with 73 Mha are close to one another. However, in season two (November–February), China has 68 Mha and India 54 Mha (Table 4). In addition, there is continuous (annual or plantation) irrigated crops of 7 Mha in China and 6 Mha in India. The AIAs are equivalent to the GIAs in the national statistics. There is no equivalent area in FAO/UF statistics to compare with the AIA. The TAAI for China is 112 Mha and for India is 101 Mha. The TAAI is equivalent to NIAs in the national statistics and 'area equipped for irrigation' in the FAO/UF study.

4.5 *Accuracies and errors*

Accuracies were determined using two independent data sets for the irrigated areas as a whole (all 28 irrigated areas put together) and for irrigated area sources: (a) major irrigation (surface water) and (b) minor irrigation (groundwater, small reservoirs and tanks). The groundtruth data provided an accuracy of 79% in mapping irrigated areas with errors of omission of 21% and commission of 23% (table 5). The Google Earth data provided an accuracy of 91%, with very low errors of omission of 9% and also low errors of commission of 16%. The accuracies for the irrigation sources (surface and groundwater) varied between 71 and 85% and the errors of omission and commission were also much higher than those of aggregated

Table 5. Accuracy assessment of IWMI GIAM V2.0. The accuracy was performed for surface water classes, ground water classes and their combinations.

	Total groundtruth sample size (number)	Correctly classified groundtruth (number)	Accuracy of irrigated area classes (%)	Errors of omissions (%)	Errors of commissions (%)
I. Accuracy based on independent groundtruth data points					
A. Surface-water and groundwater irrigated areas	1005	793	79	21	23
B. Surface-water irrigated areas	463	347	75	25	25
C. Groundwater irrigated areas	542	385	71	29	26
II. Accuracy based on independent Google Earth data points					
A. Surface-water and groundwater irrigated areas	323	295	91	9	16
B. Surface-water irrigated areas	220	187	85	15	17
C. Groundwater irrigated areas	103	79	77	23	36

irrigated area classes, mainly as a result of intermixing between the surface water and groundwater classes (table 5). The surface-water classes provided significantly higher accuracies (75–85%) when compared with groundwater classes (71–77%). Accuracies using Google Earth can be considered even better than the groundtruth data as a result of their ability to provide: (a) a spatial view of the landscape in determining irrigation at 1 km and 10 km scale, which can often be unrealistic from the ground, as discussed in the following paragraph, and (b) spatially well-distributed random points around the world.

There are a number of fundamental issues related to accuracy assessments at such large scales as 1 km or 10 km resolution pixel size. First, there are considerable difficulties in groundtruthing and establishing the exact percentage of area irrigated in a 1×1 km (100 ha), and even more so at 10×10 km (or 10 000 ha) resolutions. Take, for example, groundtruth data collected in a portion of a pixel of area of 100 ha (1×1 km). Certain portions of the 100 ha may have irrigation and certain other portions not. It is not always possible on the ground to see the entire 1×1 km to understand the representativeness of the sample site location within the pixel. Therefore, there are times that the sample site may be unrepresentative. For example, in a pixel with 40% area irrigated and the rest 'LULC,' we may have a sample site location in the LULC portion and say the pixel is non-irrigated, completely ignoring the 40% area that is irrigated. This will lead to the pixel being labelled 'other LULC' in groundtruth data, which, in reality, has 40% irrigation. Satellite sensors capture the average reflectivity from the pixel and are hence influenced by both the irrigated, as well as the non-irrigated components within the pixel, leading to average spectra for the pixel. Whereas satellite data distinctly show the difference in a pixel with zero irrigation and one with 40% irrigation, groundtruth data often fail to do so. This will lead to situations such as, for example: (a) rain-fed groundtruth points or other LULC points falling on a pixel mapped as irrigated (commission error) and (b) irrigated groundtruth points falling on a pixel mapped as other LULC (omission error). This can lead to somewhat higher omission and commission errors. The phenomenon is acute when dealing with pixels of low percentage (<30%) of irrigation, which have a greater likelihood of being labelled as classes other than irrigation, resulting in highly exaggerated errors of commission. This discussion also implies that an area-based accuracy assessment may be more powerful and robust than a point-based accuracy assessment. However, quality area-based reference data (e.g. irrigated area maps from national sources) are nearly non-existent or inconsistent for most parts of the world. Offset against this spatial advantage of remote sensing is the fact that there are multiple reasons for an average pixel-scale signal, and it is therefore possible to confound an interpretation with another reality.

In contrast, the VHRI (sub-metre to 4 m) available as 'groundtruth' from Google Earth facilitates an aerial view of the entire 100 or 10 000 ha, which will be invaluable in determining irrigation versus non-irrigation, based on a complete view of the pixel rather than a certain portion of it as in ground-based data collection. Hence, the 'zoom-in views' of the very-high-resolution Google Earth imagery are considered superior for accuracy assessment, compared to ground-based groundtruth.

5. Discussions

The discussions are divided into three main parts. First, on the evaluation of the irrigated areas obtained in this study with non-remote sensing based FAO/UF and national statistics. Second, on the study of the causes of uncertainties in the irrigated areas obtained in this study. Third, on the GIAM products and their potential applications for global food security and climate change studies.

5.1 *Evaluation of irrigated areas: GIAM versus other sources through four approaches*

The GIAM and areas obtained using remote sensing data and methods reported in this paper were evaluated using four distinct approaches. These were:

- accuracy and error assessments based on groundtruth and Google Earth data;
- comparisons with FAO/UF country-by-country statistics, which, in turn, were derived from the national statistics;
- Evaluation with India's state-by-state statistics from national sources Ministry of Water Resources (MoWR) and Central Water Commission (CWC) state-by-state statistics; and
- assessment with irrigated areas derived from finer resolution data.

It is obvious from these results and discussions why the remote sensing data and methods provide a unique perspective on irrigated areas.

5.1.1 Comparison of country-by-country irrigated areas from GIAM versus FAO/UF. The TAAI and AIA statistics are reported for 198 countries (table 4). Of these, 40 leading irrigated area countries consist of 96% of the global irrigation. The GIAM areas (table 4) were compared with: (a) an FAO/UF map (figure 10) and their statistics in FAO AQUASTAT (see a summary in the last column in table 4); and (b) national statistics (figure 11). Of the 198 countries (table 4), the GIAM areas were significantly similar (difference $<$5000 ha) to FAO/UF in 26% of the countries. In 44% of the countries, GIAM underestimates areas and in 30% of the countries GIAM overestimates areas. The GIAM TAAI in the world is 399 Mha, the equivalent of which in FAO/UF is area equipped for irrigation, which was 279 Mha. However, there is a definitive trend between GIAM and FAO/UF area (see figure 11). The combined GIAM TAAI for China and India is 102 Mha higher than the FAO/UF equipped irrigated areas. A comparison of national statistics helps explain some of these differences. For example, the official statistics of irrigated areas in India, the second leading country in irrigated areas, released by the Department of Economics and Statistics (DES) is 57 Mha (FAO AQUASTAT reports national statistics and hence has the same numbers as those of the DES). The official statistics from the DES overwhelmingly depend on the 162 major and 221 medium (major and medium commonly referred to simply as major) command areas and some other surface-water schemes.

5.1.2 Evaluation of state-by-state irrigated areas from GIAM versus national statistics for India. However, recently released minor irrigation (groundwater, small reservoirs and tanks) statistics for 2000–2001 from India's MoWR (http://mowr.gov.in/micensus/mi3census/index.htm) when combined with major and medium irrigated area statistics provide a more realistic estimate of irrigated areas. The MoWR estimates show irrigation potential utilized ($IPU_{utilized-total}$) as 84 Mha and irrigation potential created ($IPC_{created-total}$) as 111 Mha. The $IPU_{utilized-total}$ and $IPC_{created-total}$ both have intensity of cropping significantly lower than the AIA (figure 12). In China, it was demonstrated that Landsat 30 m based remote sensing estimated arable areas were 6.2 times higher than the areas estimated by the Ministry of Agriculture (Liu 2000). A 1 : 1 plot between the FAO/UF and GIAM TAAI for the 198 countries showed a slope of 0.54 and a high R^2 value of 0.94 (figure 10(*a*)). The GIAM TAAI and FAO/UF have a remarkable slope of nearly a perfect 1 (R^2=0.94) for the 154 countries (out of 198), each of which has 10 irrigated areas of 1 Mha or less (figure 10(*b*)). Of the 198 countries in figure 10(*b*), 44 were left out because the GIAM TAAI and FAO/UF had: (a) zero or near-zero irrigated areas in 37 countries and (b) huge differences in seven countries (China, India, Russia, Australia, Argentina, Kazakhstan and Iraq).

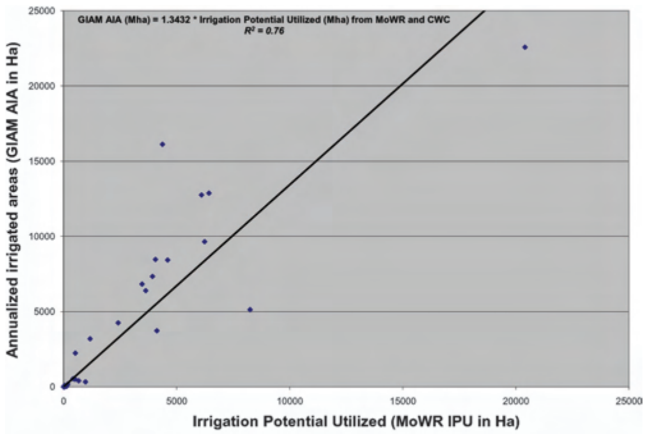

(*a*)

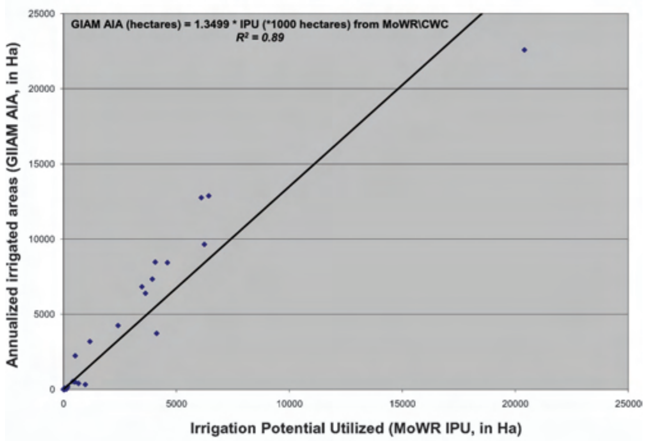

(*b*)

Figure 11. Evaluation of GIAM state-by-state irrigated areas in India with the state-by-state irrigated areas from the Indian National Statistics. The GIAM AIAs are correlated with the irrigated potential utilized (IPU) from India's Ministry of Water Resources (MoWR) and Central Water Commission (CWC) for: (a) all 33 Indian states and union territories, (*b*) 31 states and union territories after leaving out the two states with greatest discrepancy. The GIAM AIAs are also compared with irrigation potential created (IPC) from MoWR and CWC for: (*c*) all 33 Indian states and union territories and (*d*) 31 states and union territories, leaving out the two states with the greatest discrepancy. (*e*) The sum of the areas from the GIAM versus national statistics for the entire country.

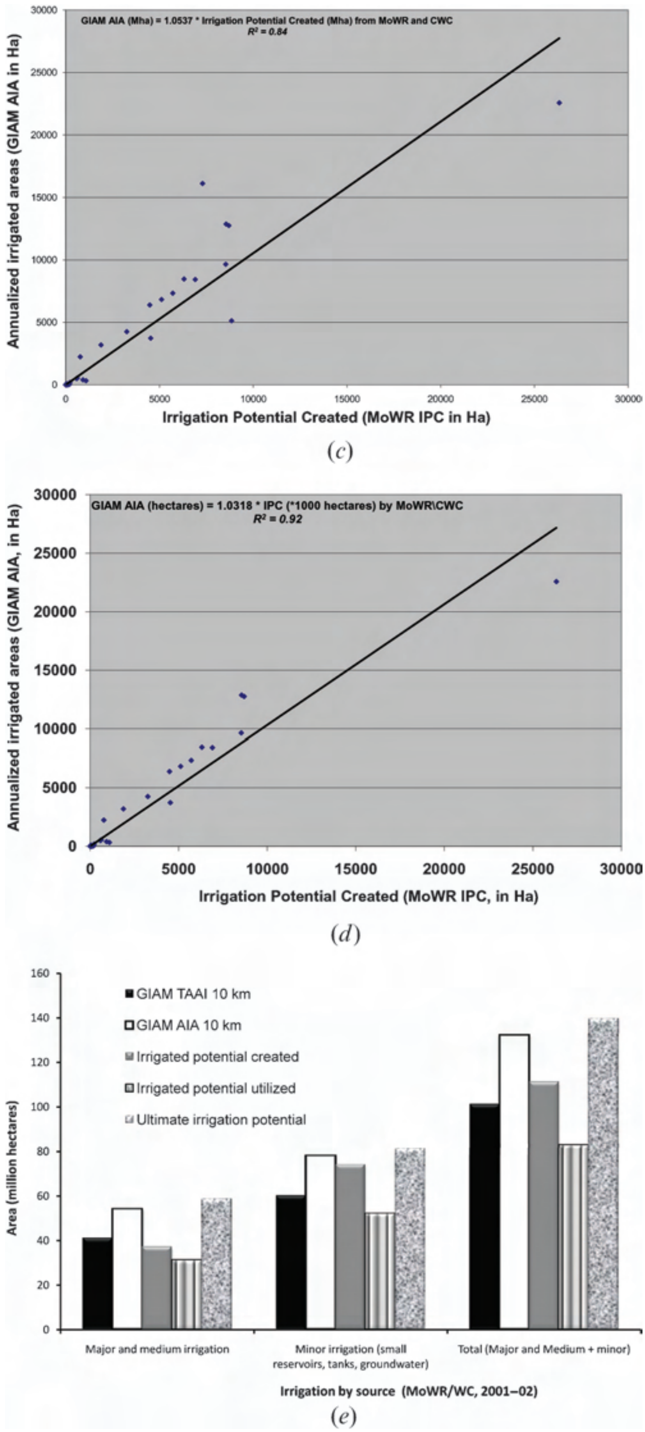

Figure 11. (*Continued.*)

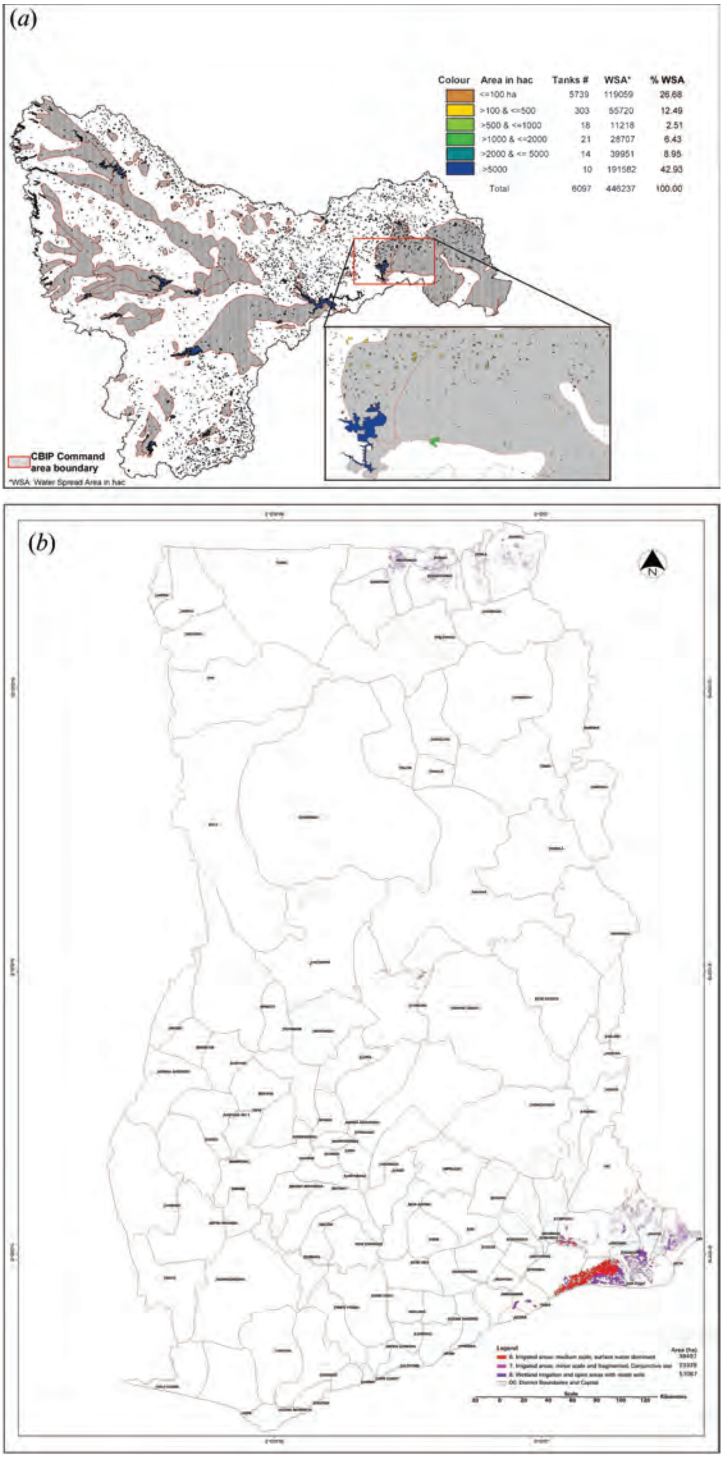

Figure 12. Validation of GIAM irrigated areas using finer resolution data. The Landsat 30 m data was used for detailed studies in (*a*) the Krishna basin and (*b*) Ghana to establish irrigated areas at 30 m. WSA: Water Spread Area in hac.

5.2 *Causes of uncertainties in irrigated areas*

The factors that influence the varying estimates of irrigated areas reported by the IWMI GIAM versus FAO/UF versus national statistics are discussed below.

5.2.1 Minor irrigation statistics are inadequately accounted for in national statistics. There is sufficient evidence that the minor irrigation (groundwater, small reservoirs and tanks) statistics are inadequately accounted for in many countries. We illustrate this for India. The DES reports India's NIAs as 57 Mha, a huge difference from the 101 Mha of the GIAM TAAI. The DES overwhelmingly depends on the 162 major and 221 medium surface-water schemes. However, recently released minor irrigation (groundwater, small reservoirs and tanks) statistics for 2000–2001 from India's MoWR (http://mowr.gov.in/micensus/mi3census/index.htm), when combined with major and medium irrigated area statistics, provide a more realistic estimate of irrigated areas. In India, the AIA estimates of various Indian states are compared with the MoWR estimates of the Indian states for: (a) $IPU_{utilized-total}$ (figures 11(*a*) and (*b*)) and (b) $IPC_{created-total}$ (figures 11(*c*) and (*d*)). First, the AIA with $IPU_{utilized-total}$ showed an R^2 value of 0.76 for a 1 : 1 line. The AIA is 1.34 times the IPU. The biggest differences were in two states: Madhya Pradesh where GIAM AIA overestimates, and Punjab, where GIAM AIA underestimates. If we leave these two states, the R^2 value goes up to 0.89. Second, the AIA with $IPU_{created-total}$ showed an R^2 value of 0.84 for a 1 : 1 line. The AIA is 1.05 times the IPC. If we leave out the two states where the differences are very high, the R^2 value goes up to 0.92. It is most appropriate to compare the AIA with the $IPU_{utilized-total}$. However, it is likely that the AIA may be picking up the $IPU_{created-total}$, given the nominal pixel size (10km $\times$ 10km). Overall, the AIA is consistently higher than areas reported in the national statistics (figure 11) as a result of the inadequate accounting of the minor irrigation (groundwater, small reservoirs and tanks). In order to prove this point, we carried out two special case studies in India and Africa using Landsat 30m data (Gumma *et al.* 2009, Velpuri *et al.* 2009). First, the Krishna basin in India showed 6097 small reservoirs (figure 12(*a*)) that, along with groundwater, irrigated 54% of all the irrigated areas, which is estimated as 9.4 Mha (Velpuri *et al.* 2009). Only 46% of the total irrigated areas of 9.4 Mha is irrigated by the 24 major reservoirs (figure 12(*a*)). The CBIP (1994) irrigated area map (see grey areas in figure 12(*a*)) almost completely ignores these smaller reservoirs, tanks and groundwater irrigation. The study involved extensive field visits. In contrast, the total known irrigated area reported for the Krishna basin is just 4.16 Mha, as calculated from the FAO/UF map. However, it is obvious from the detailed high-resolution study that the statistics are underestimated, and an area of 9.4 Mha is about the same as that determined using 500m data by Dheeravath *et al.* (2009).

Sinha (2003) also indicated irrigated areas in India to be 100 Mha. In a recent independent study, Dheeravath *et al.* (2009) used 500 m MODIS 8 day time series data of 2001–2003 for India to show the TAAI for India was 113 Mha and the AIA was 147 Mha, which are closer to the TAAI and AIA of this study. The MoWR (2005) data show that, out of 111 Mha, 74 Mha are from minor irrigation sources and 37 Mha from major irrigation sources. The GIAM TAAI estimates minor irrigation as 60 Mha and major irrigation as 41 Mha. This is mainly as a result of the growth in groundwater wells in India, estimated to vary between 19 and 26 million (Endersbee 2005). An overwhelming number of these are used for irrigation. However, the irrigated area maps and statistics on groundwater irrigation are sketchy and/or missing. Indeed, overwhelming evidence (see Shah *et al.* 2003, 2004, Endersbee 2005, MoWR 2005) shows massive overexploitation of groundwater in most of India, and the majority of the potential is already exploited. In addition, the massive exploitation of surface water from minor reservoirs is a missing link. Given these facts, it is obvious that the NIA of India far exceeds the officially reported 57 Mha, and the value is closer to 100 Mha of the TAAI reported in this study, or even slightly higher as reported by Dheeravath *et al.* (2009). The studies of Liu (2000) in China also indicate similar trends.

In Africa, the FAO/UF reports equipped irrigated areas of Ghana to be 6374 ha, whereas GIAM reported the TAAI to be 60 647 ha. The Ghanaian National statistics reports areas to be 14 699 ha (gathered from Busia, the irrigation department of Ghana). However, our case study, using Landsat 30m data (Gumma *et al.* 2009), backed by field visits showed the TAAI to be as high as 61 826 ha (e.g. figure 12(*b*)), which is about the same as reported for Ghana by the GIAM. Our field observations in Ghana also established that, if we include the supplemental irrigation of rice in the inland valley bottoms, the irrigated areas will still be higher than the 60 647 ha.

5.2.2 IAFs in GIAM may need local fractions. In this study, IAFs (Thenkabail *et al.* 2007b) were derived using three distinctly independent methods, and at least two methods were used to compute the irrigated areas: TAAI and AIA. Nevertheless, deeper understanding of each of the GIAM28 classes through groundtruths will help improve IAFs and hence irrigated areas. Computation of local IAFs, for nations and regions, instead of global IAFs are expected to help improve irrigated area classes. However, it is not clear whether local IAFs will increase or decrease the areas. The AIA is calculated based on the seasonality of every class (table 2 and figure 8(*a*)). The seasonality of a class is determined based on the NDVI time-series plot of every class.

5.2.3 Resolution influencing irrigated areas. Within the GIAM project, irrigated areas have been estimated for certain regions of the world at 500 m (Dheeravath *et al.* 2009) and 30 m (Velpuri *et al.* 2009) resolution, apart from the nominal 10 km resolution reported in this paper. A comparison of areas estimated from these different resolutions showed that the finer the resolution, the greater the area was. This is because, at finer resolution, fragmented irrigated areas, such as from groundwater, can be picked up better. Coarser resolution imagery can miss some of the fragmented irrigation, especially when the fragmented proportion is less than 40%. Ozdogan and Woodcock (2006) imply that, with coarser resolution, areas are actually higher. This is as a result of the FPA computed as actual area without using IAF and/or using a very-high area fraction when using coarser resolution imagery. Ozdogan and Woodcock also showed that the Landsat 30 m was too coarse to estimate the real extent of cultivated land in parts of China, while, for the USA, a resolution of 500 m was sufficient. However, in China, there are vast stretches of contiguous areas of irrigation, even when the field sizes are small. Therefore, even using coarse resolution imagery, these areas can be mapped with certainty. Our recent field visit to China established this fact. We use the filed visit data in an accuracy assessment. It is clear from these discussions that further studies are required to draw firm conclusions on relationships between irrigated areas and resolution of the imagery. Indications are that: (a) 'the finer the resolution, the greater is the area when irrigated areas are in fragments'. This is because in coarser resolution pixels, fragmented areas do not get accounted adequately and/or may miss out completely, resulting in underestimation of irrigated areas and (b) 'the finer the resolution, the lesser is the area in contiguous areas'. This is because, in contiguous areas, finer resolution imagery will separate out small fragments, such as settlements, roads and abandoned lands, and these areas get deducted out of the total area of fine-resolution imagery. However, in coarser resolution, smaller proportional areas, such as roads, settlements and other non-irrigated areas, get merged into larger proportional irrigated areas in the pixel, thus overestimating irrigated areas. These discussions clearly imply the need for further study in relating resolution to areas.

5.2.4 Minimum mapping unit (MMU) in determining areas. When the MMU is large (e.g. unit area is 10 000 ha), fragments of irrigated areas, such as 100 or 1 000 ha blocks, can miss out completely from being represented on a map at particular scales, such as, for example, 1 : 10 million. This will lead to miscalculations of the areas and their underestimation. We have also observed irrigated area maps that had far higher areas when the areas were calculated after digitizing, because polygons of areas are drawn as if they are contiguous units, whereas in reality, the polygons will have several LULC. In one such map, the irrigated areas of India from India's CBIP (1994) were digitized by the authors, and the area summed up to 75 Mha, whereas the statistics reported the area as 57 Mha.

It is also possible that the AVHRR off-nadir views, missing scan lines and processing for global area coverage (GAC) can also induce greater MMU than that which the pixel resolution indicates.

5.2.5 Supplemental classes. In reality, when evapo-transpiration outweighs precipitation, the only way for the crops to be sustained is through irrigation. The GIAM considers areas with significant supplemental irrigation (more than one irrigation in the crop-growing season) as an irrigated conjunctive use class (classes 16–28 in figure 8(*a*)). Often, supplemental irrigated area classes are categorized as 'rain-fed' in irrigated area maps, resulting in underestimation of irrigated areas.

5.2.6 Traditional versus remote sensing data. Traditionally, grassroots level irrigated areas observed in the field are reported next to the higher administrative unit and so on till the synthesis reaches national level. However, this type of data-gathering has many pitfalls, such as misreporting, inconsistencies in reporting as a result of the involvement of a large number of data gatherers and reporters and errors in data entry and/or synthesis. In contrast, remote sensing offers a platform of consistent data across space and time, facilitating application of consistent methods and techniques to derive irrigated area statistics.

On the other hand, time series remote sensing data potentially allow the often distinct dynamics of irrigated agriculture to stand out from other land uses, but there are many confusing situations, for instance, in the tropics, where rice may be mainly rain-fed in the monsoonal season, but receives some irrigation and is followed by one or more dry season crops, which may be completely irrigated. In tropical environments, there is generally a high degree of land cover the whole year-round and everything is 'green,' making precise definition of irrigated crops more difficult, especially if relatively coarse-scale imagery is used. Such definition issues will cause uncertainty in irrigated area estimates.

5.3 *Discussions on the methods used*

The strengths of the methods used in this paper to analyse and discern irrigated areas using remote sensing are manyfold. First, is the innovative composition of the MFDCs that facilitates analysis of multiple sensor time-series data of hundreds, or even thousands, of layers in one go. Second, the unique concept of the development of ideal spectra, based on ground knowledge from precise locations, which are then used to generate ideal spectra using time-series MFDCs. Third, development and/or adoption of unique methods, such as the SMT to group and identify classes of similar characteristics and to match class spectra with ideal (or target) spectra to help identify and label classes. Fourth, comprehensive and innovative class identification and labelling protocol that encompasses use of extensive groundtruth data, Google Earth VHRI zoom-in views (GE VHRI ZIW), BGW 2D feature space plots, ST-SC plots and time-series NDVI plots. Fifth, adoption of approaches to resolve mixed classes by using decision-tree algorithms and spatial modelling using myriad GIS data. Sixth, validation of output products using a number of approaches that include accuracies and error assessments, comparison with national statistics and use of GE VHRI ZIW. Seventh, adoption of sub-pixel irrigated area (SPIA) calculation methods that are robust and provide actual irrigated areas.

There is no single method or technique that can be successfully applied to obtain a solution to mapping irrigated areas at a global scale (Thenkabail *et al*. 2005, 2006). A suite of methods, as discussed in §2, are required. It is possible to apply other methods, such as decision-tree algorithms (DeFries *et al.* 1998) and Fourier transforms (Canisius *et al.* 2007). However, all of them have their own strengths and limitations. Initially, in the project, we did explore a number of possibilities that include decision trees, Fourier transforms and unsupervised classifications. However, the methods used in this study were innovative and powerful.

6. GIAM products and their applications

The IWMI's GIAM nominal 10 km V2.0 products are released through the web portal http://www.iwmigiam.org. The pixel resolution of the product is actually 1 km, as SPOT VGT data had that resolution. However, since the overwhelming amount of data is AVHRR 10 km, the product is referred to as 10 km. Irrigated area statistics are provided for the 198 countries (http://www.iwmigiam.org/stats). The GIAM web map server makes it possible to zoom-in to the area of interest and instantly print the dynamic and automated map composition for any country or region (http://www.iwmigiam.org/mapper.asp). Spatial spread of irrigated areas of any country in the world can be obtained instantly by calling the country from a drop-down menu. The maps are made printable with all map layout features. The GIAM map can also be uploaded onto Google Earth using the 'kmz' file (http://www.iwmigiam.org/info/main/index.asp). The portal is the place to find GIAM maps, images, method documents, area calculation procedures, posters, animations, comparisons and a host of other data and products.

The products are expected to play a key role in a number of applications, which include:

- global food security studies;
- water use/evapo-transpiration studies;

- water productivity mapping;
- inputs leading to improvements of existing global maps; and
- climate change studies.

7. Conclusions

The study developed a suite of methods and protocols for GIAM using remote sensing data. First, the study demonstrated the value of composing multiple-sensor and secondary data in a single MFDC of hundreds of data layers, akin to hyperspectral data. Second, the paper demonstrated the utility of quantitative SMTs, such as SCSs and SSVs to group, identify and label classes derived by classifying MFDCs of various segments of the world. Third, extensive standard protocols for class identification and labelling were developed to establish different types of irrigated area classes and to differentiate irrigated areas from non-irrigated areas using a hierarchical classification system. These protocols consisted of: (a) ST-SCs, (b) BGW plots, (c) Google Earth VHRI, (d) two large sources of well-distributed global groundtruth data from 5 654 locations, (e) high-resolution Landsat ETM+ mosaics, (f) time-series NDVI plots and (g) secondary data. Fourth, SPA calculation methods were introduced where SPAs were determined by multiplying IAFs by FPAs.

The study produced the first satellite-sensor-based GIAM at a nominal resolution of 10 km. This 28 class map (GIAM28) provided classes labelled based on irrigation source (e.g. surface water, groundwater or conjunctive use), intensity (e.g. single, double or continuous crop) and crop dominance. The global irrigated areas are reported for the end of the last millennium in terms of: (1) AIA and (2) TAAI. The AIA considers intensity or seasonality of irrigation and hence sums up areas irrigated during season one, season two and continuous (e.g. perennial crops or plantations or year-round crops). This is also referred to as gross area. The TAAI is the area irrigated at any given point of time plus the area equipped for irrigation but left fallow during that same period of time. This is equivalent to net area. The AIA of the world at the end of the last millennium was 467 Mha and the TAAI was 399 Mha. Of the 467 Mha AIAs, there were: (a) 252 Mha during season one, (b) 174 Mha during season two and (c) 41 Mha continuous year-round crops, such as sugarcane and plantations. Globally, irrigation by surface water was 61% and the rest (39%) by groundwater. Asia accounts for 79% (370 Mha) of all AIAs, followed by Europe (7%) and North America (7%). Three continents, South America (4%), Africa (2%) and Australia (1%), have a very low proportion of global irrigation. China and India are the two leading irrigated area countries, with a combined total of nearly 62% of the global AIAs, mainly as a result of cropping intensity (cropping during multiple seasons in a given year). Of this, China has 32.5% (152 Mha) of the global AIAs and India has 28.3% (132 Mha) of the AIAs. This is followed by the USA (5.2%), Pakistan (3.4%) and Russia (2.4%). Eight other countries (Argentina, Thailand, Bangladesh, Kazakhstan, Myanmar, Australia, Uzbekistan and Vietnam) have areas between 1 and 2% and four others (Brazil, Mexico, Indonesia and Egypt) between 0.7 and 1%. All other countries have less than 0.7% of the global AIAs. The TAAI for China is 112 Mha and for India 101 Mha. The GIAM had an accuracy of 79–91%, with errors of omission not exceeding 21%, and the errors of commission not exceeding 23%.

Accuracies were determined using two independent databases. The irrigated areas (all 28 classes put together) were mapped with an accuracy varying between 79 and

91%, with errors of omission less than 21%, and errors of commission less than 23%. Accuracies were also assessed for irrigation sources: (a) major irrigation (major and medium surface-water reservoirs) and (b) minor irrigation (groundwater, small reservoirs and tanks). Minor irrigation classes were generally more difficult to map with an accuracy of 71–77% when compared with major irrigation, which had an accuracy of 75–85%. This was mainly due to the intermixing of classes between major and minor irrigation.

Extensive comparisons were also made between the GIAM statistics with the FAO/UF and India's national statistics. The GIAM TAAI of 399 Mha was much higher than the FAO/UF areas equipped for irrigation (279 Mha). However, the GIAM TAAI and FAO/UF have a remarkable slope of a nearly perfect 1 (R^2=0.94) for the 154 countries (out of 198), each of which has 10 irrigated areas of 1 Mha or less. Detailed comparisons were also made between the GIAM statistics and India's national census data. The irrigation potential utilized ($IPU_{utilized-total}$) of India's national statistics was 84 Mha and irrigation potential created ($IPC_{created-total}$) was 111 Mha. The AIA versus $IPU_{utilized-total}$ for the 32 Indian states and union territories showed an R^2 value of 0.76 for a 1 : 1 line. The AIA was 1.34 times the $IPU_{utilized-total}$. The main causes of differences between GIAM irrigated areas, when compared with the national statistics and/or FAO/UF statistics, were due to factors such as: (a) inadequate accounting of informal minor irrigation (e.g. groundwater, small reservoirs and tanks) statistics in the national census, (b) uncertainties in IAFs in the GIAM, (c) inconsistencies in the national census data on how the irrigated areas are compiled, (d) resolutions and/or scales at which the irrigated area statistics are derived and (e) definition issues, leading to inclusion of significant supplemental irrigated areas as irrigated areas in GIAM, whereas most traditional statistics fail to do so. These are issues that need further investigation.

Particular strengths of this work were: (a) establishing AIAs that consider intensity in addition to TAAI, which does not consider intensity, (b) mapping informal minor irrigation (e.g. groundwater, small reservoirs and tanks), in addition to conventional surface-water major irrigation, (c) determining crop calendars of irrigated areas and (d) ability to simulate trends in biomass dynamics of irrigated areas over time. The possibilities for improvements exist by refining IAFs further through more intensive groundtruth and by calculating irrigated areas of every pixel by multiplying the IAF of the pixel with the FPA of the pixel in an algorithm.

The irrigated area maps and statistics for the 198 countries of the world are provided through the GIAM web portal http://www.iwmigiam.org.

Acknowledgements

The authors would like to gratefully acknowledge the support and guidance provided by Prof. Frank Rijsberman, former Director General of the IWMI. It is mainly due to his vision that a project of this complexity was possible. We would like to also thank Mr Sarath Abayawardana, former Head of the Global Research Division of the IWMI, who was instrumental in supporting the remote sensing and GIS unit initially, which later developed into a well-respected unit globally. The authors would like to thank Mr Sarath Gunasinge and Mr Ranjith Alankara for data compilation support and all the hard work relating to compilation of groundtruth data. Secretarial support from Jacintha Navaratne, Arosha Ranasinghe and Samanmali Jayathilake is much appreciated. The AVHRR pathfinder data used by the authors in this study include data produced through funding from the Earth Observing System Pathfinder Program of NASA's Mission to Planet Earth in cooperation with National Oceanic and Atmospheric Administration. The data were provided by the Earth Observing System Data and Information System (EOSDIS), the Distributed Active Archive Center at the Goddard Space Flight Center, which archives, manages and distributes this data set. This project would not have been possible without the availability of high-quality data made available for free. In this regard, we would like to thank SPOT Image (France) for SPOT VGT data, USGS for GTOPO30 and numerous other data, Dr Tim Mitchell of the CRU of the East Anglian University (UK) for precipitation data, the global rain forest mapping project (GRFM) team of NASA/JPL for the JERS-1 SAR data, the Enterprise of Google Earth visionaries in making available sub-metre to 4 m data to large parts of the world, the thousands of volunteers for the DCP, the ESRI, University of Maryland, NASA and Earth Satellite Corl. (now renamed MDA Federal Inc.) for the Landsat Geocover mosaic of the world and the global land cover facility of the University of Maryland for the forest cover map (DeFries *et al.*). Interactions, discussions and insights from the FAO/UF team (Dr Stefan Siebert *et al.*) are much appreciated. Finally, we are very grateful to our partners in China (Dr Mei Xurong and Dr Hai Weiping from the Chinese Academy of Agricultural Sciences and Dr Songcai You from the Chinese Academy of Sciences) and India (Dr Mangala Rai, Dr J.S. Samra, Dr A.K. Maji and Dr Obi Reddy of the Indian Council for Agricultural Research and Dr Bharat Sharma of the IWMI Delhi office) for making available national data, and for facilitating, support, discussions and insights. This paper is not internally reviewed by USGS Geological Survey (USGS) and hence the views expressed in this paper are not endorsed by USGS.

References

AGBU, P.A. and JAMES, M.E., 1994, *NOAA/NASA Pathfinder AVHRR Land Data Set User's Manual* (Greenbelt: Goddard Distributed Active Archive Center, NASA Goddard Space Flight Center).

AGRAWAL, S., JOSHI, P.K., SHUKLA, Y. and ROY, P.S., 2004, Spot-vegetation multi temporal data for classifying vegetation in South Central Asia. *Current Science*, **84**, pp. 1440–1448.

BARTHOLOME, E. and BELWARD, A.S., 2005, GLC2000: a new approach to global land cover mapping from Earth observation data. *International Journal of Remote Sensing*, **26**, pp. 1959–1977.

BELWARD, A.S., ESTES, J.E. and KLINE, K.D., 1999, The IGBP-DIS 1 km land cover data set DISCover: a project overview. *Photogrammetric Engineering and Remote Sensing*, **65**, pp. 1013–1020.

BIGGS, T., THENKABAIL, P.S., KRISHNA, M., GANGADHARARAO, P. and TURRAL, H., 2006, Vegetation phenology and irrigated area mapping using combined MODIS time-series, ground surveys, and agricultural census data in Krishna River Basin, India. *International Journal of Remote Sensing*, **27**, pp. 4245–4266.

BING, Z., JIANGU, L., XIANGJUN, W. and CHANGSHAN, W., 1998, Study on the classification of hyperspectral data in urban area. *SPIE*, 3502.0277-786x/98.

BIRADAR, C.M., THENKABAIL, P.S., NOOJIPADY, P., LI, Y.J., DHEERAVATH, V., VELPURI, M., TURRAL, H., GUMMA, M.K., REDDY, O.G.P., CAI, X.L., SCHULL, M.A., ALANKARA, R.D., GUNASINGHE, S., MOHIDEEN, S. and XIAO, X., 2009, A global map of rain-fed cropland areas (GMRCA) at the end of the last millennium using remote sensing. *International Journal of Applied Earth Observation and Geoinformation*, **11**, pp. 114–129.

CANISIUS, F., TURRAL, H. and MOLDEN, D., 2007, Fourier analysis of historical NOAA time series data to estimate bimodal agriculture. *International Journal of Remote Sensing*, **28**, pp. 5503–5522.

CENTRAL BOARD OF IRRIGATION AND POWER (CBIP), 1994, *Central Board of Irrigation and Power Irrigated Area Map of India for 1994* (New Delhi, India: CBIP).

COMPREHENSIVE ASSESSMENT OF WATER MANAGEMENT IN AGRICULTURE (CA), 2007, *Water for Food and Water for Life: A Comprehensive Assessment of Water Management in Agriculture*, D. Molden (Ed.) (London: Earthscan and Colombo: IWMI).

CONGALTON, R.G., 1994, Accuracy Assessment of Remotely Sensed Data: Future Needs and Directions. In *Proceedings of Pecora 12 Land Information from Space-Based Systems* (Bethesda: ASPRS), pp. 383–388.

DEFRIES, R.S. and TOWNSHEND, J.R.G., 1994, Global land cover: comparison of ground based data sets to classifications with AVHRR data. In *Environmental Remote Sensing from Regional to Global Scales*, G.M. Foody and P.J. Curran (Eds), pp. 84–110 (New York: Wiley).

DEFRIES, R., HANSEN, M. and TOWNSHEND, J., 1995, Global discrimination of land cover types from metrics derived from AVHRR Pathfinder data. *Remote Sensing of Environment*, **54**, pp. 209–222.

DEFRIES, R., HANSEN, M., TOWNSEND, J.G.R. and SOHLBERG, R., 1998, Global land cover classifications at 8 km resolution: the use of training data derived from Landsat imagery in decision tree classifiers. *International Journal of Remote Sensing*, **19**, pp. 3141–3168.

DEFRIES, R., HANSEN, M., TOWNSHEND, J.R.G., JANETOS, A.C. and LOVELAND, T.R., 2000a, *Continuous Fields 1 Km Tree Cover* (College Park, Maryland: The Global Land Cover Facility).

DEFRIES, R., HANSEN, M., TOWNSHEND, J.R.G., JANETOS, A.C. and LOVELAND, T.R., 2000b, A new global 1 km data set of percentage tree cover derived from remote sensing. *Global Change Biology*, **6**, pp. 247–255.

DHEERAVATH, V., THENKABAIL, P.S., NOOJIPADY, P., BIRADAR, C.B., TURRAL, H., CHANDRAKATHA, G., GUMMA, M., REDDY, G.P.O. and VELPURI, M., 2009, Irrigated areas of India derived using MODIS 500 m data for years 2001–2003. *ISPRS Journal of Photogrammetry and Remote Sensing* (in review).

DÖLL, P. and SIEBERT, S., 2000, A digital global irrigated area map. *ICID Journal*, **49**, pp. 55–66.

DROOGERS, P., 2002, *Global Irrigated Area Mapping: Overview and Recommendations*, Working Paper 36 (Colombo, Sri Lanka: IWMI).

EIDENSHINK, J.C. and FAUNDEEN, J.L., 1994, The 1 km AVHRR global land data set: first stages implementation. *International Journal of Remote Sensing*, **15**, pp. 3443–3462.

ENDERSBEE,, 2005, *A Voyage of Discovery: A History of Ideas About the Earth, With a New Understanding of the Global Resources of Water and Petroleum, and the Problems of Climate Change* (Frankston, Victoria, Australia: Lance Monash University Bookshop).

FARRAND, W.H. and HARSANYI, J.C., 1997, Mapping the distribution of mine tailings in the Coeur d'Alene River Valley, Idaho, through the use of a constrained energy minimization technique. *Remote Sensing of Environment*, **59**, pp. 64–76.

FLEIG, A.J., HEATH, D.F., KLENK, K.F., OSLIK, N., LEE, K.D., PARK, H., BARTIA, P.K. and GORDON, D., 1984, *User's Guide for the Solar Backscattered Ultraviolet (SBUV) and the Total Ozone Mapping Spectrum (TOMS) RUT-S and RUT-T Data Sets: October 31 1978 to November 1980*. NASA Reference Publication 1112. Report Number: NAS1.61:1112, NASA-RP-1112, REPT-910.

FOODY, G., 2002, Status of land cover classification accuracy assessment. *Remote Sensing of Environment*, **80**, pp. 185–201.

FRAMJI, K., GARG, B. and LUTHRA, S., 1981, *Irrigation and Drainage in the World*, volume I, p. 82 (New Delhi: ICID).

GRANAHAN, J.C. and SWEET, J.N., 2001, An evaluation of atmospheric correction techniques using the spectral similarity scale. In *IEEE 2001 International Geoscience and Remote Sensing Symposium*, **5**, pp. 2022–2025.

GUMMA, M.K., THENKABAIL, P., FUJII, H. and NAMARA, R., 2009, Spatial models for selecting the most suitable areas of rice cultivation in the Inland Valley Wetlands of Ghana using remote sensing and geographic information systems. *Journal of Applied Remote Sensing*, **3**, 033537.

HOLBEN, B.N., 1986, Characteristics of maximum-value composite images from temporal AVHRR data. *International Journal of Remote Sensing*, **7**, pp. 1417–1434.

HOMAYOUNI, S. and ROUX, M., 2003, Material mapping from hyperspectral images using spectral matching in urban area. Submitted to *IEEE Workshop in honour of Prof. Landgrebe*, October 2004, Washington, DC, USA.

INTERNATIONAL GEOSPHERE–BIOSPHERE PROGRAMME (IGBP), 1990, *Global Change*, Report no. 12 (Stockholm, Sweden: IGBP).

KAUTH, R.J. and THOMAS, G.S., 1976, The tasseled cap – a graphic description of the spectral–temporal development of agricultural crops as seen by Landsat. In *Proceedings of the Symposium on Machine Processing of Remotely Sensed Data*, Purdue University, West Layfayette, Indiana, pp. 4B-41–4B-50.

KIDWELL, K., 1991, *NOAA Polar Orbiter Data User's Guide* (NCDC/SDSD, Washington, DC: National Climatic Data Center).

KOGAN, F.N. and ZHU, X., 2001, Evolution of long-term errors in NDVI time-series: 1985–1999. *Advances in Space Research*, **28**, pp. 149–154.

LEICA, 2005, *Earth Resources Data Analysis System* (ERDAS Imagine 8.0) Leica Geosystems, A.G. Heinrich-Wild-Strasse, CH-9435, Heerbrugg, Switzerland.

LEICA, 2007, *Earth Resources Data Analysis System* (ERDAS Imagine8.x) Leica Geosystems, A.G. Heinrich-Wild-Strasse, CH-9435, Heerbrugg, Switzerland.

LISSENS, G., KEMPENEERS, P., FIERENS, F. and VAN RENSBERGEN, J., 2000, Development of cloud, snow, and shadow masking algorithm for VEGETATION imagery. In *Proceedings of IGARSS 2000*, Hawaii.

LIU, J.B., 2000, Study of spatial-temporal feature of modern land-use change in China: using remote sensing techniques. *Quaternary Sciences*, **20**, pp. 229–239 (in Chinese).

LOVELAND, T.R., REED, B.C., BROWN, J.F., OHLEN, D.O., ZHU, J., YANG, L. and MERCHANT, J.W., 2000, Development of a global land cover characteristics Database and IGBP DISCover from 1 km AVHRR Data. *International Journal of Remote Sensing*, **21**, pp. 1303–1330.

LOVELAND, T.R., ZHU, Z., OHLEN, D.O., BROWN, J.F., REED, B.C. and YANG, L., 1999, An analysis of the IGBP global land-cover characterization process. *Photogrammetric Engineering and Remote Sensing*, **65**, pp. 1021–1032.

MERRETT, S., 2002, *Water for Agriculture: Irrigation Agriculture in International Perspectives* . Spon's Environmental Science and Engineering Series (New York, NY: Taylor & Francis).

MINISTRY OF WATER RESOURCES (MoWR), 2005, *Third Census of Minor Irrigation Schemes (2000–2001)*. Available online at: http://mowr.gov.in/micensus/mi3census/index.htm (New Delhi: MoWR, Government of India).

MITCHELL, T.D., CARTER, T.R., JONES, P.D., HULME, M. and NEW, M., 2003, A comprehensive set of high-resolution grids of monthly climate for Europe and the globe: the observed record (1901–2000) and 16 scenarios (2001–2100). *Journal of Climate*, submitted.

NATIONAL GEOPHYSICAL DATA CENTER (NGDC), 1994, *5 Minute Gridded World Elevation*. NGDC data announcement DA 93-MGG-01 (Boulder, CO: NGDC).

OLSON, J.S., 1994a, *Global Ecosystem Framework: Definitions*. USGS EROS Data Center Internal Report (Sioux Falls, SD: USGS).

OLSON, J.S., 1994b, *Global Ecosystem Framework: Translation Strategy*. USGS EROS Data Center Internal Report (Sioux Falls, SD: USGS).

OZDOGAN, M. and WOODCOCK, C.E., 2006, Resolution dependent errors in remote sensing of cultivated areas. *Remote Sensing of Environment*, **103**, pp. 203–217.

PEUQUET, D.J. and MARBLE, D.F., 1990, *Introductory Readings in Geographic Information Systems* (New York: Taylor & Francis).

POSTEL, S., 1999, *Pillar of Sand: Can the Irrigation Miracle Last?* (New York: W.W. Norton).

RAO, C.R.N., 1993a, *Nonlinearity Corrections for the Thermal Infrared Channels of the Advanced Very High Resolution Radiometer: Assessment and Recommendations*. NOAA Technical Report NESDIS-69 (Washington, DC: NOAA/NESDIS).

RAO, C.R.N., 1993b, *Degradation of the Visible and Near-infrared Channels of the Advanced Very High Resolution Radiometer on the NOAAP9 Spacecraft: Assessment and Recommendations for Corrections*. NOAA Technical Report NESDIS-70 (Washington, DC: NOAA/NESDIS).

SAATCHI, S.S., NELSON, B., PODEST, E. and HOLT, J., 2000, Mapping land cover types in the Amazon Basin using 1 km JERS-1. *International Journal of Remote Sensing*, **21**, pp. 1201–1235.

SCHWARZ, J. and STAENZ, K., 2001, Adaptive threshold for spectral matching of hyperspectral data. *Canadian Journal of Remote Sensing*, **27**, pp. 216–224.

SECKLER, D., AMARASINGHE, U., DE FRAITURE, C., KELLER, A., MOLDEN, D. and SAKTHIVADIVEL, R. (Eds), 2000, *World Water Supply and Demand: 1995 to 2025* (Colombo, Sri Lanka: IWMI).

SHAH, T., SINGH, O.P. and MUKHERJEE, A., 2004, Groundwater irrigation and South Asian Agriculture: empirical analyses from a large-scale survey of India, Pakistan, Nepal Terai, and Bangladesh. In *IWMI-Tata Annual Partners' Meeting*, 17–19 February, Anand, India.

SHAH, T., ROY, A.D., QURESHI, A.S. and WANG, J., 2003, Sustaining Asia's groundwater boom: an overview of issues and evidence. *Natural Resources Forum*, **27**, pp. 130–140.

SHIPPERT, P., 2001, Spectral and hyperspectral analysis with ENVI. ASPRS ENVI user's group notes. In *Annual Meeting of the American Society of Photogrammetry and Remote Sensing*, 22–28 April, St. Louis, Missouri, USA.

SIEBERT, S., FEICK, S. and HOOGEVEEN, J., 2005a, A digital global map of irrigation areas – an update for Asia. In *Frankfurt Hydrology Paper 01* (Germany: Frankfurt University).

SIEBERT, S., HOOGEVEEN, J. and FRENKEN, K., 2006, Irrigation in Africa, Europe, and Latin America. Update of the Digital Global Map of Irrigation Areas to Version 4. In *Frankfurt Hydrology Paper 05* (Germany: University of Frankfurt).

SIEBERT, S., DÖLL, P., HOOGEVEEN, J., FAURES, J.-M., FRENKEN, K. and FEICK, S., 2005b, Development and validation of the global map of irrigation areas. *Hydrology and Earth System Sciences*, **9**, pp. 535–547.

SINHA, S., 2003, Rs 24,500 cr plan for harvesting rain water. *Times of India*, 6 January 2003.

SMITH, P.M., KALLURI, S.N.V., PRINCE, S.D. and DEFRIES, R.S., 1997, The NOAA/NASA Pathfinder AVHRR 8 km land data set. *Photogrammetric Engineering and Remote Sensing*, **63**, pp. 12–31.

THENKABAIL, P.S., GANGADHARARAO, P., BIGGS, T., KRISHNA, M. and TURRAL, H., 2007a, Spectral matching techniques to determine historical land use/land cover (LULC) and irrigated areas using time series AVHRR Pathfinder Data sets in the Krishna River Basin, India. *Photogrammetric Engineering and Remote Sensing*, **73**, pp. 1029–1040.

THENKABAIL, P.S., BIRADAR, C.M., NOOJIPADY, P., CAI, X.L., DHEERAVATH, V., LI, Y.J., VELPURI, M., GUMMA, M. and PANDEY, S., 2007b, Sub-pixel irrigated area calculation methods. *Sensors Journal, Special Issue: Remote Sensing of Natural Resources and the Environment*, **7**, pp. 2519–2538, Available online at: http://www.mdpi.org/sensors/papers/s7112519.pdf.

THENKABAIL, P.S., SCHULL, M. and TURRAL, H., 2005, Ganges and Indus River Basin land use/land cover (LULC) and irrigated area mapping using continuous streams of MODIS data. *Remote Sensing of Environment*, **95**, pp. 317–341.

THENKABAIL, P.S., ENCLONA, E.A., ASHTON, M.S. and VAN DER MEER, V., 2004a, Accuracy assessments of hyperspectral waveband performance for vegetation analysis applications. *Remote Sensing of Environment*, **91**, pp. 354–376.

THENKABAIL, P.S., ENCLONA, E.A., ASHTON, M.S., LEGG, C. and JEAN DE DIEU, M., 2004b, Hyperion, IKONOS, ALI, and ETM+ sensors in the study of African rain forests. *Remote Sensing of Environment*, **90**, pp. 23–44.

THENKABAIL, P.S., BIRADAR, C.M., TURRAL, H., NOOJIPADY, P., LI, Y.J., VITHANAGE, J., DHEERAVATH, V., VELPURI, M., SCHULL, M., CAI, X.L. and DUTTA, R., 2006, *An Irrigated Area Map of the World (1999) Derived From Remote Sensing*, Research report 105 (IWMI). Available online at: http://www.iwmigiam.org.

TOMLIN, D., 1990, *Geographic Information Systems and Cartographic Modeling* (New Jersey: Prentice Hall College Division).

TOMLINSON, R., 2003, *Thinking About Geographic Information Systems Planning for Managers* (California: ESRI Press).

TOU, J.T. and GONZALEZ, R.C., 1975, *Pattern Recognition Principles* (Reading, Massachusetts: Addison-Wesley Publishing Company).

TUCKER, C.J., GRANT, D.M. and DYKSTRA, J.D., 2005, NASA's global orthorectified Landsat data set. *Photogrammetric Engineering and Remote Sensing*, **70**, pp. 313–322.

US GEOLOGICAL SURVEY (USGS), 1993, *Digital Elevation Models, Data User Guide 5* (Reston, Virginia: USGS).

VAN SCHILFGAARDE, J., 1994, Irrigation – a blessing or a curse. *Agricultural Water Management*, **25**, pp. 203–219.

VELPURI, M., THENKABAIL, P.S., GUMMA, M.K., BIRADAR, C.B., DHEERAVATH, V., NOOJIPADY, P. and YUANJIE, L., 2009, Influence of resolution or scale in irrigated area mapping and area estimations. *Photogrammetric Engineering and Remote Sensing*, accepted, in press.

VERDIN, K. and JENSON, S., 1996, Development of continental scale DEMs and extraction of hydrographic features. In *Proceedings of the Third Conference on GIS and Environmental Modeling* (Santa Fe, New Mexico: NCGIA).

VERDIN, K.L. and GREENLEE, S.K., 1996, Development of continental scale digital elevation models and extraction of hydrographic features. In *Proceedings of Third International Conference/Workshop on Integrating GIS and Environmental Modeling*, Santa Fe, New Mexico, 21–26 January 1996 (Santa Barbara, CA: National Center for Geographic Information and Analysis).